# Factors Controlling Black Carbon Distribution in the Arctic

Ling Qi[1,2], Qinbin Li[1,2], Yingrui Li[3], Cenlin He[1,2]

[1]Department of Atmospheric and Oceanic Sciences, University of California, Los Angeles, CA, USA
[2]Joint Institute for Regional Earth System Science and Engineering, University of California, Los Angeles, CA, USA
[3]School of Physics, Peking University, Beijing, China

*Correspondence to*: Ling Qi (qiling@atmos.ucla.edu)

**Abstract**. We investigate the sensitivity of black carbon (BC) in the Arctic, including BC concentration in snow ($BC_{snow}$, ng $g^{-1}$) and surface air ($BC_{air}$, ng $m^{-3}$), to emissions, dry deposition and wet scavenging using a global 3-D chemical transport model (CTM) GEOS-Chem. We find that the model underestimates $BC_{snow}$ in the Arctic by 40% on average (median = 11.8 ng $g^{-1}$). Natural gas flaring substantially increases total BC emissions in the Arctic (by ~70%). The flaring emissions lead to up to 49% increases (0.1−8.5 ng $g^{-1}$) in Arctic $BC_{snow}$, dramatically improving model comparison with observations (50% reduction in discrepancy) near flaring source regions (Western Extreme North of Russia). Ample observations suggest that BC dry deposition velocities over snow and ice in current CTMs (0.03 cm $s^{-1}$ in GEOS-Chem) are exceedingly small. We apply the resistance-in-series method to compute the dry deposition velocity ($v_d$) that varies with local meteorological and surface conditions. The resulting velocity is significantly larger and varies by a factor of eight in the Arctic (0.03–0.24 cm $s^{-1}$), increases the fraction of dry to total BC deposition (16% to 25%), yet leaves the total BC deposition and $BC_{snow}$ in the Arctic unchanged. This is largely explained by the offsetting higher dry and lower wet deposition fluxes. Additionally, we account for the effect of the Wegener-Bergeron-Findeisen (WBF) process in mixed-phase clouds, which releases BC particles from condensed phases (water drops and ice crystals) back to the interstitial air and thereby substantially reduces the scavenging efficiency of BC (by 43−76% in the Arctic). The resulting $BC_{snow}$ is up to 80% higher, BC loading is considerably larger (from 0.25 to 0.43 mg $m^{-2}$), and BC lifetime is markedly prolonged (from 9 to 16 days) in the Arctic. Overall, flaring emissions increase $BC_{air}$ in the Arctic (by ~20 ng $m^{-3}$), the updated $v_d$ more than halves $BC_{air}$ (by ~20 ng $m^{-3}$), and the WBF effect increases $BC_{air}$ by 25−70% during winter and early spring. The resulting model simulation of $BC_{snow}$ is substantially improved (within 10% of the observations) and the discrepancies of $BC_{air}$ are much smaller during snow season at Barrow, Alert and Summit (from -67%−-47% to -46%−3%). Our results point toward an urgent need for better characterization of flaring emissions of BC (e.g. the emission factors, temporal and spatial distribution), extensive measurements of both the dry deposition of BC over snow and ice, and the scavenging efficiency of BC in mixed-phase clouds. In addition, we find that the poorly constrained precipitation in the Arctic may introduce large uncertainties in estimating $BC_{snow}$. Doubling (halving) precipitation introduces a positive (negative) bias similar as the magnitude of the overall effects of flaring emissions and the WBF effect.

## 1. Introduction

BC (loosely also known as soot), light absorbing refractory carbonaceous aerosols, influence climate through direct absorption of solar radiation, semi-direct cloud effects, indirect cloud effects, and snow-albedo effect (Bond et al., 2013; IPCC, 2014). BC deposited on surfaces with high albedo, such as snow and ice, reduces surface albedo (the so-called snow albedo effect), increases surface solar heating, and accelerates snow and ice melting (Flanner et al., 2007, 2012; He et al., 2014b; Liou et al., 2014). This snow albedo feedback leads to enhanced BC radiative forcing (Bond et al., 2013 and references therein). Warren and Wiscombe (1985) highlighted the climate effect of fallen soot from 'smokes' for a nuclear war scenario, which reduced the

surface reflectivity of snow and sea ice in the Arctic. Measurements by Clarke and Noone (1985) showed that there was ample amount of BC in the Arctic snow to exert climate impacts in the region. Using observations of $BC_{snow}$, Hansen and Nazarenko (2004) quantified, for the first time, the albedo reduction due to BC deposition on snow and ice (2.5% on average) across the Arctic. Snow albedo effect of BC in the Arctic has since received wide attention. Numerous studies have examined the snow albedo change in this region due to BC deposition (Jacobson, 2004; Marks and King, 2013; Namazi et al., 2015; Tedesco et al., 2016) and estimated the associated surface BC snow albedo radiative forcing to be substantial (0.024–0.39 W $m^{-2}$) in the Arctic (Bond et al., 2013 and references therein; Flanner, 2013; Jiao et al., 2014; Namazi et al., 2015), comparable to the forcing of tropospheric ozone in springtime Arctic (0.34 W $m^{-2}$, Quinn et al., 2008). BC deposited on snow and ice is likely to be an important reason for unexpected rapid sea ice shrinkage in the Arctic (Koch et al., 2009; Goldenson et al., 2012; Stroeve et al., 2012). Widespread surface melting of the Greenland ice sheet was attributed to rising temperatures and reductions in surface albedo resulting from deposition of BC from Northern Hemispheric forest fires (Keegan et al., 2014; Tedesco et al., 2016).

To better constrain the radiative forcing and the associated uncertainties of BC snow albedo effect in the Arctic, it is imperative to improve the prediction of $BC_{snow}$ in the region. Previous studies found large discrepancies between modeled and observed $BC_{snow}$ (up to a factor of six) in the Arctic (e.g. Flanner et al., 2007; Koch et al., 2009). A comprehensive survey of $BC_{snow}$ observations across the Arctic (~1000 snow samples) by Doherty et al. (2010) provides a unique opportunity to constrain $BC_{snow}$ in the region. Bond et al. (2013) compared results of $BC_{snow}$ from the Community Atmospheric Model (CAM version 3.1) (Flanner et al., 2009) and the Goddard Institute of Space Studies (GISS) model (Koch et al., 2009) with the observations from Doherty et al. (2010), averaged over the eight Arctic sub-regions (Fig. 1) as defined by Doherty et al. (2010). The resulting ratio of modeled to observed $BC_{snow}$ (sub-regional means) were 0.6−3.4 for CAM3.1 and 0.3−1.6 for GISS. Jiao et al. (2014) found large discrepancies in $BC_{snow}$ (up to a factor of six) between results from the Aerosol Comparisons between Observations and Models (AeroCom, http://aerocom.met.no/) and the Doherty et al. (2010) observations. They also found large variations in BC deposition fluxes among the AeroCom models. Jiao et al. (2014) further pointed out that BC transport and deposition processes are more important for differences in simulated $BC_{snow}$ than differences in snow meltwater scavenging rates or emissions in models.

Studies have shown that Arctic atmospheric BC on average cools the surface due to surface dimming, while BC in the lower troposphere warms the surface with a climate sensitivity (surface temperature change per unit forcing) of 2.8 ± 0.5 K $W^{-1}$ $m^2$ due to low clouds and sea-ice feedbacks that amplify the warming (e.g. Flanner, 2013). This sensitivity is a factor of two larger than that of BC snow albedo feedback (1.4 ± 0.7 K $W^{-1}$ $m^2$, Flanner, 2013), a factor of four larger than that of $CO_2$ (0.69 K $W^{-1}$ $m^2$, Bond et al., 2013) and much larger than that of tropospheric ozone (0.2 K $W^{-1}$ $m^2$, Shindell et al., 2009). However, estimates of $BC_{air}$ in the Arctic are associated with large uncertainties (Textor et al., 2006, 2007; Koch et al., 2009; Liu et al., 2011; Browse et al., 2012; Sharma et al, 2013). In general, current models successfully reproduced the decadal declining trends observed at surface sites Barrow, Alert and Zeppelin (Sharma et al., 2004, 2006, 2013; Eleftheriadis et al., 2009), but failed to reproduce the seasonal cycles of $BC_{air}$ observed at the aforementioned sites, with large underestimates during Arctic haze season (Textor et al., 2006, 2007; Koch et al., 2009; Liu et al., 2011; Browse et al., 2012; Sharma et al, 2013; Eckhardt et al., 2015). Specifically, mean $BC_{air}$ during January to March was underestimated by about a factor of 2 for the mean of all models, although the discrepancy is up to a factor of 27 for individual models (Eckhardt et al., 2015). The low biases are likely due to uncertainties associated with estimates of BC emissions in Russia (Huang et al., 2015), treatments of BC aging in the models (Liu et al., 2011; He et al., 2016), excessive dry deposition of BC (Huang et al., 2010; Liu et al., 2011), wet scavenging of BC (Koch et al., 2009;

Huang et al., 2010; Bourgeois and Bey, 2011; Liu et al., 2011), or overly efficient vertical mixing (Koch et al., 2009). Studies (Wang et al., 2011; Huang et al., 2015) pointed out that the low biases of $BC_{air}$ during Arctic haze season are partially due to uncertainties in the estimates of BC emissions in Russia, resulted from biases in both BC emission rates and spatial distributions. A likely missing source of BC emissions in Russia is natural gas flaring emissions, most of which cluster in in the Western Extreme North of Russia (Stohl et al., 2013). Although in totality gas flaring emissions are a rather small fraction of global BC emissions, their proximity to the Arctic can conceivably result in disproportionately large impact. Dry deposition of BC on snow and ice is yet another poorly understood and quantified process. Observations show that $v_d$ over snow and ice covered surfaces vary by orders of magnitude (0.01–1.52 cm $s^{-1}$; Hillamo et al., 1993; Bergin et al., 1995; Nilsson and Rannik, 2001; Grönlund et al., 2002; Held et al., 2011; Wang et al., 2014). Current chemical transport models tend to assume uniform and low dry deposition velocities over such surfaces to capture the high surface $BC_{air}$ during the Arctic haze season (Wang et al., 2011; Sharma et al., 2013). For instance, Wang et al. (2011) used a uniform $v_d$ of 0.03 cm $s^{-1}$ over snow and ice and found a better comparison with $BC_{air}$ measurements during the Arctic haze season. However, this value is probably too low for snow-covered land surfaces with larger roughness length. Additionally, observations show that BC scavenging efficiency varies from 0.06 to 0.7 depending on liquid water contents, temperature, and ice mass fraction because of the WBF process in mixed-phase clouds (Cozic et al., 2007; Verheggen et al., 2007). However, in most of the current AeroCom models, BC scavenging is poorly treated (Wang et al., 2011; Bourgeois and Bey, 2011) or entirely missing (Liu et al., 2011) in mixed-phase clouds, which cover the Arctic in ~40% of the time through a whole year (Zhang et al., 2011). For example, BC scavenging in mixed-phase clouds was treated the same as that in warm clouds in GEOS-Chem (Wang et al., 2011). In ECHAM5-HAM2, BC scavenging efficiency in mixed-phase clouds was set up as 0.06, the lowest observed value in those clouds (Bourgeois and Bey, 2011).

Constraining individual processes of BC is often challenging. As such, our focus is more geared toward highlighting missing processes or ones that were previously unaccounted for in governing BC in the Arctic, particularly BC deposition in the region. We first examine and incorporate gas flaring emissions of BC, which was missing in previous emission estimates yet account for a large fraction of BC emissions in the Arctic as suggested by Stohl et al. (2013) (Sect. 4.1). We then discuss and improve simulation of $v_d$ of BC over snow and ice, which varies by orders of magnitude but was treated as a uniform value by previous studies (Sect. 4.2). We then analyze BC wet scavenging efficiency in mixed-phase clouds accounting for effects of WBF (Sect. 4.3). Finally, we estimated the sensitivity of $BC_{snow}$ to precipitation in the Arctic (Sect. 4.4). We also use $BC_{air}$ as an additional constrain of these simulations.

## 2. BC observations in the Arctic

### 2.1 Measurements of BC in snow

The most comprehensive measurements of $BC_{snow}$ were in eight sub-regions in the Arctic: Alaska, Arctic Ocean, Canadian Arctic, Canadian sub-Arctic, Greenland, Russia, Ny-Ålesund and Tromsø, mostly from March to May during 2005–2009 (Doherty et al., 2010; data available at http://www.atmos.washington.edu/sootinsnow/). Samples were for full snowpack depth and the sampling sites are shown in Fig. 1 (color coded by the sub-regions). These observations provide a reasonable constraint on Arctic-wide annual mean radiative effect from BC deposited in snow (Jiao et al., 2014).

Doherty et al. (2010) measured the light absorption of impurity in snow samples using the Integrating Sphere/Integrating Sandwich optical method and derived equivalent, maximum, and estimated $BC_{snow}$ using the wavelength-dependent absorption of

BC and non-BC fractions (Doherty et al., 2010). We use here the estimated $BC_{snow}$. The largest sources of uncertainty stem from uncertainties of BC mass absorption cross-section (MAC), BC absorption Ångstrom exponent ($Å_{BC}$), and non-BC absorption Ångstrom exponent ($Å_{non-BC}$) constituents. Doherty et al. (2010) used MAC = 6.0 $mg^2$ $g^{-1}$ (at 500 nm), the MAC of their calibration filters. Using MAC = 7.5 $mg^2$ $g^{-1}$ (at 500 nm) as recommended by Bond and Bergstrom (2006) would increase the estimated $BC_{snow}$ by ~25%. Doherty et al. (2010) used $Å_{BC}$ = 1.0 (range: 0.8–1.9) and $Å_{non-BC}$ = 5.0 (range: 3.5–7.0) in their derivation and estimated a 50% error in the estimated $BC_{snow}$. Additional uncertainties include instrumental uncertainty (≤ 11%), under-catch correction (±15%), and loss of aerosol to plastic flakes in the collection bags (±20%) for samples from West Russia and the Canadian sub-Arctic. The overall uncertainty of the estimated $BC_{snow}$ is < 60%.

**2.2 Measurements of BC in surface air**

In-situ measurements of $BC_{air}$ from 2007 to 2009 are available at five sites within the Arctic Circle (Fig. 1): Denali, AL (63.7°N, 149.0°W, 0.66 km a.s.l.), Barrow, AL (71.3°N, 156.6°W, 0.01 km a.s.l.), Alert, Canada (82.3°N, 62.3°W, 0.21 km a.s.l.), Summit, Greenland (72.6°N, 38.5°W, 3.22 km a.s.l.), and Zeppelin, Norway (79°N, 12°E, 0.47 km a.s.l.). Data descriptions are shown in Table 1. Denali is part of the Interagency Monitoring of PROtected Visual Environment (IMPROVE) network (Malm et al., 1994; data available at http://vista.cira.colostate.edu/improve/). IMPROVE measurements are made every three days and 24-hour averages are reported. Thermal Optical Reflectance (TOR) combustion method is used based on the preferential oxidation of organic carbon (OC) and BC at different temperatures (Chow et al., 2004). BC-like products of OC pyrolysis can lead to an overestimate of the BC mass. The uncertainties of the TOR method are difficult to quantify (Park et al., 2003; Chow et al., 1993).

Barrow is part of the NOAA Global Monitoring Division (GMD) network, where BC light absorption coefficients are measured from a particle soot absorption photometer (PSAP) since 1997 (Bond et al, 1999; Delene and Ogren, 2002; data available at http://www.esrl.noaa.gov/gmd/aero/net/). PSAP measures the change in light transmission at three wavelengths (467, 530 and 660 nm) through a filter on which particles are collected. We used the measurements at 530 nm in this study. Site Barrow is about 8 km northeast of the village of Barrow and is less than 3 km southeast of the Arctic Ocean. Given that the site has a prevailing east-northeast wind off the Beaufort Sea, it receives minimal influence from local anthropogenic emissions and is strongly affected by weather in the Central Arctic.

$BC_{air}$ at Alert were measured using an aethalometer model AE-6 with 1-wavelength operated by Environment Canada (Sharma et al., 2004; 2006; 2013; data available at http://www.ec.gc.ca/). The instruments measure the attenuation of light transmitted through particles that accumulate on a quartz fiber filter at 880nm. Alert, located the furthest north of the five sites on the north-eastern tip of Ellesmere Island, is most isolated from continental sources (Hirdman et al., 2010).

The Zeppelin observatory is part of the European Supersites for Atmospheric Aerosol Research, where BC mass concentrations are also measured by an aethalometer and reported for seven wavelengths (370, 470, 520, 590, 660, 880 and 950 nm) (Eleftheriadis et al., 2009; data available at http://ebas.nilu.no/). We use the 520 nm data. Measurements at site Zeppelin, on mountain Zeppelin in island archipelago of Svalbard, were generally considered to represent the free troposphere conditions (Eleftheriadis et al., 2009).

BC mass concentrations were also measured by an aethalometer at Summit (von Schneidemesser et al., 2009; data available at

http://www.esrl.noaa.gov/gmd/aero/net/), on the center of the Greenland glacial ice sheet. Due to the high elevation (3.2 km) and the flat and homogeneous terrain around (Hirdman et al., 2010), measurements at Summit are representative for the Arctic free troposphere.

The uncertainty of filter-based absorption measurements of BC (PSAP and aethalometer) lies in empirical corrections of the overestimated absorption if light transmission is also affected by particulate light scattering (Bond et al., 1999). Accuracy of this correction is 20–30% (Delene and Ogren, 2002; Weingartner et al., 2003; Virkkula et al., 2005). Additional uncertainty results from the empirical conversion from optical response to BC mass using an assumed mass absorption cross-section (MAC), which depends on the composition and morphology of the particles used in the calibration of the instrument and on the specific technique used to quantify the BC mass (Clarke et al., 1987; Slowik et al., 2007). The MAC of BC varies by up to a factor of four (5–20 $m^2$ $g^{-1}$) (Weingartner et al., 2003). We use 9.5 $m^2$ $g^{-1}$ for station Barrow at wavelength 530 nm as recommended for the ARCTAS period (McNaughton et al., 2011; Wang et al., 2011). The MAC used at Alert (Sharma et al., 2013), Zeppelin (Eleftheriadis et al., 2009) and Summit (Hagler et al., 2007) are 19 $m^2$ $g^{-1}$, 15.9 $m^2$ $g^{-1}$ and 20 $m^2$ $g^{-1}$. The uncertainty of absorption enhancement by non-BC absorbers (organic carbon and mineral dust) is generally difficult to quantify unless the non-BC absorbers contribute more than 40% of absorption (Petzold et al., 2013).

## 3. Model description and simulations

### 3.1 GEOS-Chem simulation of BC

GEOS-Chem is a global 3-D chemical transport model driven with assimilated meteorology from the Goddard Earth Observing System (GEOS) of the NASA Global Modeling and Assimilation Office (GMAO). GEOS-5 meteorological data set are used to drive model simulation at 2° lat × 2.5° lon resolution and 47 vertical layers from the surface to 0.01 hPa. Tracer advection is computed every 15 min with a flux-form semi-Lagrangian method (Lin and Rood, 1996). Tracer moist convection is computed using GEOS convective, entrainment, and detrainment mass fluxes as described by Allen et al. (1986a, b). Deep convection is parameterized using the relaxed Arakawa-Schubert scheme (Moorthi and Suarez, 1992; Arakawa and Schubert, 1974), and the shallow convection treatment follows Hack (1994). BC aerosols are emitted by incomplete fossil fuel and biofuel combustion and biomass burning. We use global BC emissions from Bond et al. (2007) with updated emissions in Asia from Zhang et al. (2009). Biomass burning emissions are from the Global Fire Emissions Database version 3 (GFEDv3) (van der Warf et al., 2010) with updates for small fires in Randerson et al. (2012). It is assumed that 80% of the freshly emitted BC aerosols are hydrophobic (Park et al., 2003) and are converted to hydrophilic with an e-folding time of 1.15 days, which yields a good simulation of BC export efficiency in continental outflow (Park et al., 2005). Dry deposition in the model is computed using a resistance-in-series method (Wesely, 1989; Zhang et al., 2001), whereas it assumes a constant aerosol $v_d$ of 0.03 cm $s^{-1}$ over snow and ice (see Sect. 3.3). Wet deposition follows Liu et al. (2001), with updates as described in Wang et al. (2011).

### 3.2 Gas flaring emissions of BC

Gas flaring is the controlled burning of natural gas in petroleum producing areas, particularly in areas lacking gas transportation infrastructure (Elvidge et al., 2009; 2011). It is estimated that 3.5% of world's natural gas is flared (Elvidge et al., 2016) and results in a large amount of green house gas emissions (13,662.6 Gg of $CO_2$, Bradbury et al., 2015). Stohl et al. (2013) derived BC emissions from gas flares by multiplying gas flaring volumes by emission factors. The flaring volumes were estimated using

low light imaging data acquired by the Defense Meteorological Satellite Program (DMSP) (Elvidge et al., 2011). The DMSP estimates of flared gas volume are based on a calibration developed with a pooled set of reported national gas flaring volumes and data from individual flares. Stohl et al. (2013) derived BC emission factor based upon emission factors of particulate matter from flared gases. The resulting gas flaring emissions (228 Gg $yr^{-1}$) accounts for ~5% of global anthropogenic emissions (4.8 Tg $yr^{-1}$, Bond et al., 2007) and ~3% of global total emissions (8.5 Tg $yr^{-1}$, including anthropogenic emissions from Bond et al. (2007) and Zhang et al. (2009) and biomass burning emissions from Randerson et al., 2012). However, the largest contributor Russia, contributing ~30% to the global flaring volume, locates in the clean Arctic Circle. About 40% of BC emissions in the Arctic (115 Gg $yr^{-1}$) are from gas flaring (48 Gg $yr^{-1}$), shown in Fig. 1. It is estimated that flaring emissions contribute 42% to the annual mean $BC_{air}$ at surface in the Arctic (Stohl et al., 2013). However, to our knowledge, no study so far has investigated the contribution of flaring emissions to $BC_{snow}$ in the Arctic. Thus, we included flaring emissions from Stohl et al. (2013, data on flaring emissions is available at http://eclipse.nilu.no upon request) and investigated the contribution of flaring emissions to $BC_{snow}$ and $BC_{air}$ in the Arctic in Experiment B (Table 2).

### 3.3 Dry deposition over snow and ice

Nilsson and Rannik (2001) conducted eddy-covariance flux measurements of aerosol number dry deposition in the Arctic Ocean and found a mean $v_d$ of 0.19 cm $s^{-1}$ over open sea, 0.03 cm $s^{-1}$ over ice floes and 0.03−0.09 cm $s^{-1}$ over leads (Table 3). Following Nilsson and Rannik (2001), Fisher et al. (2011) imposed $v_d$ = 0.03 cm $s^{-1}$ for aerosols over snow and ice. They found improved agreements of simulated sulfate with in-situ observations in spring and winter in the Arctic. Wang et al. (2011), also imposing $v_d$ = 0.03 cm $s^{-1}$ for aerosols over snow and ice, found better agreements for BC at the same stations as used by Fisher et al. (2011). They thus recommended a uniform $v_d$ = 0.03 cm $s^{-1}$ for sulfate and BC over snow and ice. To capture the winter and spring haze, other studies also used relatively low $v_d$ = 0.01–0.07 cm $s^{-1}$ (Liu et al., 2011; Sharma et al., 2013). These low values, however, are likely too small for snow-covered land surface, where larger roughness lengths reduce the aerodynamic resistance thereby increase $v_d$ (Gallagher et al., 2002). The roughness length is 0.005 m for sea ice and 0.03−0.25 m for snow-covered land surface with grass and scattered obstacles (Wieringa, 1980). As a result, $v_d$ is larger over snow-covered land surface than over sea ice. Observed values over snow and ice are 0.01–2.4 cm $s^{-1}$ for aerosol particles in general and 0.01–1.52 cm $s^{-1}$ for BC in particular (Table 3). Again, this suggests that a uniform value of $v_d$ = 0.03 cm $s^{-1}$ is problematic. We apply the resistance-in-series method to calculate $v_d$ of BC over snow and ice, as a function of aerodynamic resistance, particle density and size and surface types (Experiment C, Table 2).

We would like to note that most of these observations (Held et al., 2011; Nilsson and Rannik, 2001; Bergin et al., 1995) were from summertime Arctic (June−August) and clean regions (e.g., the Arctic Ocean and Greenland) far from anthropogenic pollutions. In addition, most of the $v_d$ measurements are for general aerosol particles. The only available dry deposition velocities specific to BC particles are derived from the strong surface enhancement of $BC_{snow}$ between two snow events at Mt. Changbai (42.5°N, 128.5°E, 0.74 km) in Northern China (Table 3). Wang et al. (2014) derived $v_d$ = 0.16−1.52 cm $s^{-1}$. Despite uncertainties from sublimation (Wang et al., 2014), these measurements suggest that the low $v_d$ used in previous studies (Fisher et al., 2010; Liu et al., 2011; Wang et al., 2011; Sharma et al., 2013) might underestimate the role of dry deposition during snow season, particularly near source regions. Wang et al. (2014) concluded that dry deposition in the boundary layer may dominate over wet deposition (a factor of five larger) during dry season in some regions, particularly near source regions with high $BC_{air}$. It is thus imperative to obtain measurements of $v_d$ of BC in polluted regions in Russia and Northern Europe in spring, when radiative forcing associated with BC snow-albedo effect is maximum (Flanner et al., 2013).

### 3.4 Wegener-Bergeron-Findeisen (WBF) process in mixed-phase clouds

Most AeroCom models (Textor, 2006) parameterize rainout rate following Giorgi and Chameides (1986). The rainout ratio is proportional to precipitation formation rate and mass mixing ratio of BC in condensed phase in clouds, which is determined by the scavenging efficiency of BC ($r_{scav.}$),

$$r_{scav.} = \frac{[BC]_{condensed}}{[BC]_{interstitial} + [BC]_{condensed}} , \quad (1)$$

where $r_{scav.}$ is the scavenging efficiency and quantifies the partition of BC aerosols between condensed phase and the interstitial air; $[BC]_{condensed}$ is the mass mixing ratio of BC in condensed phase, including water drops and ice crystals in clouds, $[BC]_{interstitial}$ is the mass mixing ratio of BC in the interstitial air.

Hygroscopicity and size of BC-containing particles are determining factors for $r_{scav}$ (Sellegri et al., 2003; Hallberg et al., 1992, 1995). Internal mixing with soluble inorganic species enhances the $r_{scav}$ for aged BC particles (Sellegri et al., 2003). For instance, $r_{scav}$ is 0.39±0.16 for BC-containing particles with diameter smaller than 0.3 μm and a small fraction (38%) of soluble inorganic material. It increases to 0.97±0.02 for particles with diameter larger than 0.3 μm and a larger fraction (57%) of soluble inorganic material (Sellegri et al., 2003). In addition to particle properties, cloud microphysics and dynamics play a significant role in determining $r_{scav}$ of BC in mixed-phase clouds (Hitzenberger et al., 2000, 2001; Cozic et al., 2007; Hegg et al., 2011). Measured $r_{scav}$ of BC decreased from 0.60 in liquid only clouds to 0.05–0.10 in mixed-phase clouds, a reduction of more than a factor of five (Cozic et al., 2007; Henning et al., 2004; Verheggen et al., 2007). Such reduction was attributed to the effect of the WBF process (Cozic et al., 2007). In mixed-phase clouds, ice crystals grow at the expense of water drops when the environmental vapor pressure is higher than the saturation vapor pressure of ice crystals but lower than the saturation vapor pressure of water droplets (Wegener, 1911; Bergeron, 1935; Findeisen, 1938). As such, BC-containing particles in the water drops are released back to the interstitial air and consequently $r_{scav}$ is reduced. Another process, riming (Hegg et al., 2011), in mixed-phase clouds has an opposite effect on BC scavenging. When ice particles fall and collect the water drops along the pathway, the snow particles show rimed structure and the scavenging efficiency remains the same. Riming rate is determined by the terminal velocity of snowflakes, ice crystals and liquid water contents (LWC) in clouds (Fukuta et al., 1999).

Previously, only the hygroscopicity of BC containing particles is considered in BC $r_{scav}$ in models (Wang et al., 2011, and references therein). It is typically assumed that 100% of hydrophilic BC particles are readily incorporated into cloud drops and all hydrophobic BC particles remain in the interstitial air in warm and mixed-phase clouds. This treatment of mixed-phase clouds as liquid phase is likely to overestimate $r_{scav}$ in mixed-phase clouds. In models that include mixed-phase clouds, assumptions still need to be made about $r_{scav}$. A uniform scavenging efficiency (0.4 or 0.06) for all mixed-phase clouds has been imposed (Stier et al., 2005; Bourgeois and Bey, 2011), while observations show that BC scavenging efficiency varies dramatically with temperature and ice mass fraction (Cozic et al., 2007; Henning et al., 2004; Verheggen et al., 2007).

In Experiment D (Table 2), we discriminate WBF- vs. riming-dominated conditions and parameterize BC scavenging efficiency under the two conditions separately in mixed-phase clouds (248 K < T < 273 K, Garrett et al., 2010). We assume that riming dominates when temperature is around -10°C (261 K < T < 265 K) and LWC is above 1.0 g $m^{-3}$, following Fukuta et al. (1999). The WBF process dominates otherwise. Our parameterization of the effect of the WBF process on BC scavenging efficiency is based on the measurements at Mt. Jungfraujoch (46.4°N, 8°E, 3.85 km), an elevated mountainous site far from pollution sources

and regularly engulfed in clouds (30% of the time) (Cozic et al., 2007). We evaluated the effects of WBF on global BC distribution and tested the sensitivity of the simulation to the switch temperature from warm clouds to mixed-phase clouds and from mixed-phase clouds to ice clouds in a companion study (Qi et al., 2016). In this study, we focus on the effects of WBF on BC distribution in the Arctic.

### 3.5 BC concentration in snow

In snow models, such as SNICAR, the initial surface $BC_{snow}$ is defined as the ratio of BC deposition to snow precipitation (Flanner et al., 2007). Here we approximate $BC_{snow}$ using BC deposition flux and snow precipitation rate, following Kopacz et al. (2011), Wang et al. (2011) and He et al. (2014a):

$$[BC_{snow}] = \frac{F_{BCdep}}{F_{snow}} = \frac{F_{wet\_dep} + F_{dry\_dep}}{F_{snow}} \quad , \tag{2}$$

where $F_{BC,dep}$, $F_{wet\_dep}$ and $F_{dry\_dep}$ are total, dry and wet deposition flux of BC and $F_{snow}$ the snow precipitation. The top and bottom snow depth of each sample are provided in the observation dataset (Doherty et al., 2010). The top and bottom snow depths of each sample and the collection date are provided in the observation dataset (Doherty et al., 2010). We accumulate snow precipitation (GEOS-5) in the model from the collection date backward until the modelled snow depths, respectively, reach the observed top and bottom depths of the snow sample, then the two dates are stored. We use the average BC deposition fluxes and snow precipitation between the two dates to estimate the $BC_{snow}$ for the sample. The rate of snow accumulation at the surface is estimated as snow precipitation flux (kg $m^{-2}$ $s^{-1}$) over snow density (kg $m^{-3}$). The observed annual average snow density is 300 kg $m^{-3}$ over the Arctic basin, increasing from 250 kg $m^{-3}$ in September to 320 kg $m^{-3}$ in May with little geographical variation across the Arctic (Warren et al., 1999; Forsström et al., 2013). We use the annual average snow density in the estimate.

The above estimate of $BC_{snow}$ ignores many processes that may alter the BC snow concentrations, such as wind-redistribution of surface snow, sublimation, and melt water flushing (Doherty et al., 2010, 2013; Wang et al., 2013). Wind-redistribution of surface snow is a sub-grid scale phenomenon. Except for turbulent scale wind direction and strength, small-scale topography also plays an important role in surface snow redistribution. So this process is really difficult to simulate by global models. Precipitation rate and relative humidity in much of the Arctic are low, so in some areas appreciable (up to 30-50%) surface snow is lost to sublimations (Liston and Sturm, 2004). $BC_{snow}$ at surface can thus be underestimated by our method. We filtered snow samples collected during melting season, so the melt water flushing has little effect on our estimate.

To reduce the biases in comparison of model results and observations, we organize the observations as follows: (1) Observations from March to May in 2007-2009 are used while those from June to August are excluded, because our estimate of $BC_{snow}$ does not resolve snow melting; (2) We exclude observations with obvious dust or local wood-burning contaminations as described in Doherty et al. (2010); (3) We average the observations in the same model grid and snow layer and collected on the same day.

Table 2 summarizes various model simulations in the present study. Experiment A is the standard case. We include gas flaring emissions in Experiment B (Sect. 3.2). Contrasting Experiments B and A thus offer insights to the contribution of gas flaring emissions on BC in the Arctic. Experiment C includes the updated $v_d$ (Sect. 3.3). The difference of Experiment B and C denote the effects of updated $v_d$ to BC distribution. Experiment D includes temperature-based WBF parameterization (Sect. 3.4). The

effects of WBF to BC in the Arctic are shown by the difference of Experiment C and D. Additional simulations are described where appropriate.

## 4. The effects of gas flares, dry deposition, WBF and precipitation

We discuss the effects of gas flaring emissions, dry deposition, WBF in mixed-phase clouds, and precipitation on BC distribution in the Arctic in this section. The probability density function (PDF) of observed and GEOS-Chem simulated $BC_{snow}$ in the Arctic is approximately lognormal (Fig. 2(a)). The arithmetic mean of observations is 17.4 ng $g^{-1}$, larger than the geometric mean of 12.7 ng $g^{-1}$ and the median of 11.8 ng $g^{-1}$ (see the vertical lines in Fig. 2 and Table 1). The model reproduces the observed distribution, but underestimates $BC_{snow}$ by 40% (Experiment A). By including flaring emissions (Sect. 4.1), updating $v_d$ (Sect. 4.2) and including WBF in mixed-phase clouds (Sect. 4.3), the discrepancy is reduced to -10%. Gas flaring emissions lower the discrepancy from -40% to -20% (Experiment B). The updated $v_d$ (Experiment C) makes insignificant changes to $BC_{snow}$ in the Arctic. WBF (Experiment D) further reduces the discrepancy from -20% to -10%. The resulting $BC_{snow}$ in the eight sub-regions agree with observations within a factor of two. This discrepancy is acceptable for global models because it has been suggested that the error due to different spatial sampling of global models (~200 km) and point observations was up to 160% (Schutgens et al., 2016). In addition, $BC_{air}$ at surface and in the free troposphere is sensitive to the above three processes in the Arctic, particularly during winter and spring (see Sects. 4.1–4.3).

### 4.1 Gas flaring emissions

Gas flaring emissions increase total BC emissions by 67% (from 0.068 to 0.115 Tg $yr^{-1}$) in the Arctic Circle (60°N and higher latitudes), resulting in a 19% increase of the total BC deposition (from 0.32 to 0.38 Tg $yr^{-1}$). Flaring emissions increase $BC_{snow}$ (by 0.1−8.5 ng $g^{-1}$) in the eight Arctic sub-regions. The higher $BC_{snow}$ leads to significant reduction in the negative biases (by 20–100%), except in the Arctic Ocean and in Tromsø, where $BC_{snow}$ is already overestimated without flaring emissions (Fig. 3). $BC_{snow}$ in Greenland is not affected by gas flaring emissions. The reason is two-folded: first, snow samples in Greenland are far from the flares in Western Russia; second, the vertical transport of BC from surface to the upper troposphere is suppressed by the stable atmosphere in the Arctic (Stohl, 2006), resulting in negligible effect of flaring emissions to $BC_{snow}$ over Greenland (above 1.5 km).

The largest enhancement of $BC_{snow}$ from flaring emissions is in the Western Extreme North of Russia within the Arctic Circle (by 5.0 ng $g^{-1}$ on average, or, 50%), which reduces model discrepancy substantially across Russia (from -50% to -30%). However, simulated $BC_{snow}$ is now too high by a factor of two near the flares (observed value ~19.3 ng $g^{-1}$). The overestimate is likely because of excessively large flaring emission estimates. Yet $BC_{snow}$ is too low by a factor of two in far fields (observed value ~30.7 ng $g^{-1}$), despite a large increase (by 50%, from 10.5 to 15.5 ng $g^{-1}$) as a result of flaring emissions.

Flaring emissions are assumed to be proportional to flared gas volumes and emission factors. Errors in estimates of flared volumes in Russia is small (within ±5%, Elvidge et al., 2009). Estimates of emission factors, on the other hand, are known to have several orders of magnitude uncertainties (Schwarz et al., 2015; Weyant et al., 2016). Given limited observations of BC emission factors from actual flares, Stohl et al. (2013) derived BC emission factor based upon emission factors of particulate matter from flared gases. They used a BC emission factor of 1.6 g $m^{-3}$, which is more than a factor of three higher than that (0.5 g $m^{-3}$) from a lab experiment on fuel mixtures typical in the oil and gas industry (McEwen et al., 2012). Recent field measurements

have suggested an even lower emission factor (0.13±0.36 g $m^{-3}$) from ~30 individual flares in North Dakota, with an upper bound of 0.57 g $m^{-3}$ (Schwarz et al., 2015; Weyant et al., 2016). These studies found that average BC emission factors for individual flares varied by two orders of magnitude, and furthermore, two flares from the same flare stack that were resampled on different days showed different BC emission factors (Weyant et al., 2016). They also pointed out that emission factors are not correlated with ambient temperature, pressure, humidity, flared gas volumes or gas composition. It is thus imperative that extensive measurements of BC emission factors be made in the flare regions.

Yet another source of uncertainty is flare stack height, which is not accounted for in current flaring emission estimates. Typical stack heights vary from 15 to 250 m, sometimes above the nighttime boundary layer eight of 150−300 m in the Arctic (Di Liberto et al., 2012). The stack height affects the ventilation, dispersion, deposition, and long-range transport of the emissions. For example, local deposition of BC may be suppressed and downwind long-range transport enhanced when the stacks emitted BC in the free troposphere (Chen et al., 2009). The lack of proper treatment of flare stack height in the model may partially explain the aforementioned discrepancies of modeled $BC_{snow}$ (biased high in Western Russian and low in Eastern Russia). Another factor for the underestimate of $BC_{snow}$ in Eastern Russia is likely local sources, such as domestic wood burning in nearby villages and fishing camps, diesel trucks on highway and coal burning in a power plant, that are unaccounted for in the emission inventory (Doherty et al., 2010, Fig. 1). Although we filter out samples with strong local contamination, it is conceivable that local emissions still add to the background $BC_{snow}$ in Eastern Russia.

Jiao et al. (2014) have shown that most AeroCom models underestimated $BC_{snow}$ in Russia and pointed to the flaring emissions as a likely cause. Our model results show that even with flaring emissions, which are likely on the high side, $BC_{snow}$ is still too low (by 50%) in Eastern Russia. Therefore, there are likely other factors such as the lack of local emissions in Eastern Russia, weak dry deposition fluxes (Sect. 4.2), and excessively low rate of sublimation of surface snow, that contribute to the large model discrepancy in $BC_{snow}$.

Fig. 4 shows observed and GEOS-Chem simulated daily $BC_{air}$ from January to March at Zeppelin, a site that is closest to the gas flares in the Western Extreme North of Russia. The inclusion of flaring emissions captures some of the large spikes in the observed $BC_{air}$, such as those from late February to March in 2008 and in January 2009. Stohl et al. (2013) found that flaring emissions captured observed large spikes at Zeppelin during a transport event in February 2010 with a high BC/CO ratio, a signature of gas flaring emissions (CAPP, 2007). The inclusion of flaring emissions results in enhanced $BC_{air}$, for instance, in February 2007 and in January 2008, that are not seen in the observations. This is largely from the lack of temporal variation of flaring emissions (Weyant et al., 2016). The temporal variation is, however, difficult to characterize based on the current knowledge of flaring emissions in the Western Extreme North of Russia (Stohl et al., 2013). Flaring emissions also increase $BC_{air}$ during snow season (Sep. to Apr.) (by 16−19 ng $m^{-3}$) at Barrow and Alert, resulting in substantial reductions of discrepancies (from -47% to -15% at Barrow and -67% to -46% at Alert) (Fig. 5). Flaring emissions are transported to the high Arctic within the Arctic dome by efficient circumpolar transport (Stohl, 2006). The effect of flaring emissions at Denali in low Arctic is negligible, because the site is outside of the cold Arctic front (around 65−70°N in Alaska) (Barrie, 1986; Ladd and Gajewski, 2010), which is a strong barrier for the meridional transport of BC (Stohl, 2006). $BC_{air}$ at Summit (3.22 km a.s.l.), which is mostly in the free troposphere, is not affected by flaring emissions, either. This is because the vertical transport of BC is suppressed by the stable atmosphere during snow season in the Arctic (Stohl, 2006).

### 4.2 Dry deposition velocity

It is known that $v_d$ of aerosol particles over snow and ice surfaces strongly depend on particle size, surface types and meteorological conditions and vary by orders of magnitude (Table 3). We estimate $v_d$ of BC particles as a function of particle properties, aerodynamic resistance and surface types (Sect. 3.3). The results over the Arctic Ocean and Greenland are shown in Table 3, generally within the observed range. At Mt. Changbai, model result of BC $v_d$ (0.09−0.14 cm $s^{-1}$) is an order of magnitude lower than that derived by Wang et al. (2014) (0.16−1.52 cm $s^{-1}$). The resulting dry deposition fluxes are lower than observations by a factor of five. We attribute the large discrepancies to two factors. First, the point measurements were at a mountainous site with complex terrain and micro-meteorological conditions. Neither can be resolved in a global model (He et al., 2014a). Second, the values reported by Wang et al. (2014) were estimated from relative enhancements of surface $BC_{snow}$ between two snow events. These estimates are known to have large uncertainties (a factor of two) from the measured sublimation fluxes and the assumption of snow density (Wang et al., 2014).

Compared to the results of uniform $v_d$ of 0.03 cm $s^{-1}$ over snow and ice, the updated $v_d$ leads to larger dry deposition fluxes, a larger fraction of dry over total deposition, and relatively unchanged total deposition fluxes. Simulated mean BC $v_d$ in the eight Arctic sub-regions (Fig. 1) are 0.03–0.14 cm $s^{-1}$, considerably larger that the uniform value of 0.03 cm $s^{-1}$ over snow and ice (Table 5). Correspondingly, the $v_d$ are 19−195% larger in most sub-regions, with the largest increase in Greenland (by 195%) and over Russia (by 87%) (Table 5). We find that BC dry deposition flux is more sensitive to $v_d$ in source regions (e.g., Russia) than in remote regions, reflecting the high $BC_{air}$ in the former. A comparable increase in $v_d$ of BC (from 0.03 cm $s^{-1}$ to 0.08 cm $s^{-1}$) in Russia and Alaska results in vastly different increases in BC dry deposition flux (87% in Russia versus 30% in Alaska). As expected, larger dry deposition flux depletes $BC_{air}$ thereby reducing wet deposition flux but offsets the reduction in wet deposition. As a result, both total deposition flux and $BC_{snow}$ remain relatively unchanged (< 5%) in the eight sub-regions, except in Ny-Ålesund and Tromsø. In these last two regions, the total deposition fluxes are 10−15% smaller. The lower deposition fluxes reflect efficient removal of BC aerosols over source regions. BC in Ny-Ålesund and Tromsø are primarily from Europe and Russia, transported isentropically in cold season (Stohl, 2006; Eleftheriadis et al., 2009). Rapid dry deposition in these source regions results in enhances boundary layer removal hence lower BC loadings in air and a reduced boundary layer outflow (Liu et al., 2011).

The change in the fraction of dry to total deposition has important implications for BC radiative forcing in the Arctic. The fraction increases from 19% (7−33%) to 26% (14−41%), by 14−73%, with the largest increase in Russia (from 23% to 40%) where BC deposition flux and $BC_{snow}$ are the largest in the Arctic (Tables 4 and 5). Typically, BC particles removed by dry deposition are externally mixed with snow particles, while those removed by wet deposition are internally mixed with snow particles (Flanner et al., 2009, 2012). Internal mixing of BC with snow/ice particles increases the absorption cross-section of BC/snow composites by about a factor of two (Flanner et al., 2012). The enhanced absorption further increases the snow albedo radiative forcing (He et al., 2014b). It is thus conceivable that the larger dry deposition fraction will lead to less internally mixed BC/snow composite and lower snow albedo radiative forcing. This effect is critical before melting season, because melting might quickly eliminates the differences in the mode of BC deposition. Other post-depositional processes include wind-driven drifting and sublimation (Doherty et al., 2013). The former does not change the fraction of external and internal mixing of BC with snow. The later might expose BC particles in the internally mixed BC/snow composite out and reduce the fraction of internally mixed BC/snow composite. Yet this process occurs slowly in a relatively long time.

Unlike $BC_{snow}$, $BC_{air}$ is a strong function of $v_d$, particularly during snow season. With updated $v_d$, model results fail to capture the seasonal cycle of $BC_{air}$ with dramatic decreases during snow season (by 20−23 ng $m^{-3}$, 27−68%) at Barrow, Alert, and Zeppelin (Fig. 5). The decreases at Barrow and Alert are a direct result of larger dry deposition in the boundary layer because of substantially larger $v_d$ (0.07 cm $s^{-1}$, Table 5). At Zeppelin (in Ny-Ålesund), where $v_d$ is only marginally higher (17%), the large reduction of $BC_{air}$ (~40%) is largely attributed to the suppressed transport from proximate source regions in Europe and Russia. This dramatic decrease of $BC_{air}$ in winter with larger $v_d$ and the lack of winter and spring Arctic haze is one of the major reasons of using low $v_d$ in previous studies (Wang et al., 2011; Sharma et al., 2013; Liu et al., 2011). However, this does not justify the use of a low $v_d$ over snow and ice. First, observations have shown very large variations of $v_d$ (Table 3), which suggest that a uniform representation might involve large uncertainties. Second, observations of $v_d$ over snow and ice show very large values in certain region, which is still underestimated by the resistance-in-series method. Third, besides dry deposition in boundary layer, $BC_{air}$ is affected by a lot of other factors, such as emissions, transport and wet deposition (Sect. 4.3).

**4.3 WBF in mixed-phase clouds**

Our model results show that WBF increases $BC_{snow}$ by 20−80% in the eight Arctic sub-regions, except Canadian sub-Arctic, and increases $BC_{air}$ during snow season by 25−70% (Figs. 2 and 7). Clearly WBF suppresses the scavenging of BC in mixed-phase clouds and consequently enhances poleward transport. We validate the simulation of WBF and the associated effects on global BC distribution in a companion study (Qi et al., 2016).

WBF not only increases $BC_{snow}$ in the Arctic but also changes the partition of dry and wet deposition of $BC_{snow}$. Intuitively WBF slows down wet scavenging, thus allowing more BC particles available for dry deposition. Our results show that the fraction of dry to total deposition increases from 26% (12−41%) to 35% (19−59%) on average in the eight Arctic sub-regions, thereby lowering the absorption of solar radiation due to less internally mixed BC-snow composite (Sect. 4.2). In Alaska, Canadian Arctic and Russia, BC removed by dry deposition increases to more than 50%. However, averaged globally, this fraction increases only slightly (from 19% to 20%), indicating that the fraction in the Arctic is more sensitive to the WBF effect.

The scavenging efficiency of BC, heretofore defined as the fraction of BC incorporated in cloud water drops or ice crystals in mixed-phase clouds, is strongly affected by WBF and as a result varies temporally and spatially in response to varying temperature (Sect. 3.3). Thus, improved treatment of mixed-phase cloud processes, such as WBF and riming, is essential to improve the simulation of spatial and temporal distribution of BC. BC in Alaska and the Canadian Arctic are most sensitive to the WBF effect in the Arctic. WBF increases $BC_{snow}$ by 55% in Alaska and 43% in the Canadian Arctic and reduces the model discrepancies to within 10% (Table 4 and Fig. 3). $BC_{air}$ at Barrow in Alaska and at Alert in Canadian Arctic are higher by 20−30 ng $m^{-3}$ in winter, reducing the model discrepancies significantly (from -54% to -18% at Barrow and from -72% to -46% at Alert) and enhancing the seasonal variation (Fig. 5). Similar improvements are also seen at Summit in Greenland, where $BC_{air}$ increases by 12 ng $m^{-3}$ and the model discrepancy lowers significantly (from -48% to 3%). This is consistent with recent observations, which showed that high riming rate was rare (12%) in the North American sector of the Arctic and that WBF dominated in-cloud scavenging in mixed-phase clouds (Fan et al., 2011).

At Zeppelin where snow samples show rimed structures (Hegg et al., 2011), model discrepancy of $BC_{air}$ increases to 63% from -10% with the WBF effect included. Model results do not capture the magnitude of $BC_{air}$ in winter at Barrow, Alert and Zeppelin (Fig. 5). $BC_{air}$ is well simulated at Zeppelin but underestimated at Barrow and Alert in Experiment A. $BC_{air}$ is well simulated at

Barrow and Alert but overestimated at Zeppelin in Experiment D (Fig. 5) – similar results were shown in Sharma et al. (2013). Such apparent discrepancy can be partly attributed to the fact that models do not properly distinguish WBF-dominated in-cloud scavenging at Barrow (Fan et al., 2011) and riming-dominated scavenging at Zeppelin (Hegg et al., 2011). Here we separate WBF- and riming-dominated conditions based on temperature and LWC (Sect. 3.3, and Fukuta et al., 1999) in Experiment D. However, model results still fail to capture the difference among the three sites. There are a number of reasons. First, LWC from GEOS-5 biased high compared to CloudSat observations (Barahona et al., 2014). In addition, the spatial distribution of LWC from GEOS-5 also has large discrepancy (Li et al, 2012; Barahona et al., 2014). Second, this separation is based on a laboratory experiment, while conditions in the real atmosphere are much more complex. Therefore, more field measurements are required to better separate the two conditions and better parameterize BC scavenging efficiency.

Our results show that WBF exaggerates the positive bias of $BC_{air}$ in summer and delays the transition from the late-spring haze to the clean summer boundary layer (Experiment D). Previous studies found that the dominant process controlling low summertime aerosol at Barrow is the onset of local wet scavenging by warmer clouds (Garrett et al., 2010, 2011). WBF suppresses scavenging in mixed-phase clouds and thus slows down the onset of strong scavenging by warmer clouds during the transition from winter to summer. However, the strong scavenging of warm drizzling clouds in late spring and summer boundary layer (Browse et al., 2012), which enhances the winter-summer transition, is not considered in the present study. At high latitudes in summer, low stratocumulus cloud decks in the boundary and lower troposphere produce frequent drizzle (90% of the time) and remove aerosols effectively (Browse et al., 2012).

### 4.4 Precipitation

We compute $BC_{snow}$ as the ratio of BC deposition flux to precipitation rate (Sect. 3.5). It has been pointed out that this estimate is very sensitive to uncertainties in precipitation (He et al., 2014a). Climatological precipitation across the Arctic is 14.3 g $cm^{-2}$ $yr^{-1}$ for 1965–89 (Overland and Turet, 1994) and is 16.3 g $cm^{-2}$ $yr^{-1}$ for 1971–91 (Serreze et al., 1995) as constrained from observed hydrologic budget (Warren et al., 1999). The annual precipitation, averaged for 2007–09, is 15.5 g $cm^{-2}$ $yr^{-1}$ in GEOS-5, within the range of the observations. There are considerable uncertainties, spatially and temporally, in precipitation in the Arctic (Warren et al., 1999; Serreze et al., 2000). Fig. 6 compares monthly precipitation from the Global Precipitation Climatology Project (GPCP, Huffman et al., 2001), NOAA Climate Prediction Center Merged Analysis of Precipitation (CMAP, Xie and Arkin, 1997), and GEOS-5. The discrepancies can be as large as a factor of 10 and the seasonal cycles are largely out of phase between the three datasets. Specifically, GPCP precipitation is much stronger than CMAP, particularly during summer. GEOS-5 precipitation is within the range of GPCP and CMAP data. The exception is Greenland, Ny-Ålesund, and Tromsø, where GEOS-5 precipitation is substantially (a factor of 2–10) larger than GPCP and CMAP data during the snow season. Snow precipitation in the Arctic is difficult to constrain for two reasons. First, accurate measurements of snowfall in the Arctic have proven nearly impossible, because snow gauges strongly under-catch snowfall (by 55−75%) depending on the gauge type and wind condition (Liston and Sturm, 2004). Second, a more fundamental problem is that the sparse observational network in the Arctic is vastly inadequate to accurately estimate the monthly mean precipitation (Serreze et al., 2000) – 10–40 stations are required in 2.5° grid cells (WCRP, 1997).

To probe the sensitivity of BC deposition and $BC_{snow}$ to precipitation, we conduct two additional model simulations, where we halve and double precipitation rate in the Arctic, with other processes configured as in Experiment D. We find that, in GEOS-5, during the snow season, nearly all precipitation is in the form of snow in the Arctic. Halving precipitation leads to increases in

$BC_{snow}$ by 15−136%, with largest enhancements in Greenland (136%) and Ny-Ålesund (92%) (Fig. 7). With precipitation halved, it takes a longer accumulation time for a given snow depth, which results in larger dry deposition (up to 153% increases). As such, the ratio of BC dry deposition to snow precipitation increases as well. On the other hand, the ratio of BC wet deposition to snow precipitation, determined mainly by in-cloud scavenging of BC, remains largely unchanged. Overall, $BC_{snow}$ increases with halved precipitation. It is conceivable that doubled precipitation has the opposite effect. Indeed, $BC_{snow}$ decreases by 14−43% in the eight Arctic sub-regions. In addition, dry deposition decreases by 35−62% and the fraction of dry to total deposition decreases by 23−43%. Although $BC_{snow}$ as computed here is sensitive to precipitation, the resulting medians of $BC_{snow}$ in the eight sub-regions are in agreement with observations within a factor of two, except over Greenland (a factor of five too high) and Tromsø (a factor of three too high). Further analysis of the results at Greenland and Tromsø is in Sect. 4.5. The strong sensitivity of $BC_{snow}$ calls for better constraining of precipitation in the Arctic.

In contrast, annual BC burden and deposition are much less sensitive to precipitation. Halving Arctic precipitation increases annual BC burden by 12% and decreases annual BC deposition by 16% in the Arctic. This is because less precipitation removes fewer BC particles. BC lifetime in the Arctic, as determined by the BC burden and deposition, increases by 27%. When precipitation is doubled, annual BC burden decreases by 14%, while BC deposition increases by 8%, resulting in a 23% reduction of BC lifetime in the Arctic.

$BC_{air}$ is more sensitive to precipitation at Barrow, Alert and Zeppelin than at Denali and Summit (Fig. 8). When precipitation is halved, annual $BC_{air}$ increases by 20−70% at Alert, by 10−40% at Barrow and Zeppelin, and by 1−20% at Denali and Summit. When precipitation is doubled, annual $BC_{air}$ decreases by 20−50% at Alert, by 10−40% at Barrow and Zeppelin, and by 2−20% at Denali and Summit. Additionally, $BC_{air}$ is more sensitive to precipitation in summer than in winter. This is because the summer clean boundary layer in the Arctic is controlled by strong local scavenging (Garrett et al., 2010, 2011; Browse et al., 2012).

**4.5 BC in snow in Greenland, Tromsø and Canadian sub-Arctic**

$BC_{snow}$ is associated with much larger uncertainties over short (hence shallower snow depth) than longer (hence larger snow depth) time periods. Because snow samples over Greenland were collected at the very surface (~0 cm), the computed $BC_{snow}$ thus represents BC deposition only through the duration of a day for direct comparisons. The short time duration thus largely explains the larger uncertainties in the estimated $BC_{snow}$. In Tromsø, observed $BC_{snow}$ were considerably lower (19.1 ng $g^{-1}$) from samples collected over a clean mountain plateau upwind of town Tromsø (Doherty et al., 2010) and much higher (53.3 ng $g^{-1}$) from samples collected in town (Forsström et al. 2013). We use the former for comparisons. Thus, the factor of two overestimate of $BC_{snow}$ in this region is because that GEOS-Chem does not resolve sub-grid variability.

In the Canadian sub-Arctic, $BC_{snow}$ is underestimated by 50% with all the improvements discussed above (Experiment D). This large low bias is mainly from the low $BC_{snow}$ in the subsurface samples (1−20 cm, 11.7 ng $g^{-1}$, ~60% of all samples), accumulated through the snow season. $BC_{snow}$ in this region increases by 33% from flaring emissions and by 43% from halving precipitation. Yet the resulting $BC_{snow}$ is still 25% lower than observations (12.8 ng $g^{-1}$). However, GEOS-5 precipitation is at the lower end among the three precipitation datasets (Fig. 6). The large discrepancy in $BC_{snow}$ warrants further studies.

## 5. Discussions

Global BC emissions in this study are within the range of previous studies, but emissions in the Arctic (0.115 Tg $yr^{-1}$) exceed the higher end of those used in previous studies (0.037−0.077 Tg $yr^{-1}$, Table 6). The large Arctic emissions in this study result from gas flares, which have been missing in previous estimates. It has been suggested that gas flares are a dominant BC source in the Arctic – it is 42% of the total BC emissions in the Arctic, but a rather small fraction (3%) of the global BC emissions (Stohl et al., 2013). Although this estimate is probably biased high because of the large emission factor (Sect. 4.1), it does not justify that we should exclude these emissions in modelling BC.

BC deposition in the Arctic (0.38 Tg $yr^{-1}$) exceeds the higher end of those used in previous studies (0.13–0.34 Tg $yr^{-1}$) with flaring emissions included (Table 6). Our model results suggest that annual BC deposition in the Arctic is more sensitive to BC emissions and precipitation rate in the region than $v_d$ and WBF. Flaring emissions increases BC deposition flux in the Arctic by 19%. Doubling (halving) precipitation in the Arctic increases (decreases) BC deposition by 8% (18%). Total BC emissions in the Arctic is a factor of two to five lower than the total BC deposition, suggesting that a large fraction of BC deposited in the Arctic is from long-range transport.

Simulation of $BC_{snow}$ in this study is much better than most of the AeroCom models in the perspective of mean model bias across the Arctic (Experiment D in this study: -0.8 ng g-1; AeroCom models: -13.2 – +21.4 ng g-1, Table 6) and the biases for the eight sub-regions (Experiment D in this study: a factor of 2; AeroCom estimates: a factor of 5−6, Jiao et al., 2014). In addition, the correlation coefficient of modeled and simulated $BC_{snow}$ in this study (0.21) locates at the higher end of previous AeroCom estimates (0.12−0.24). We find that flaring emissions improve the agreement of $BC_{snow}$ with observations significantly, with a 50% reduction to the negative bias of modeled $BC_{snow}$ across the Arctic and a substantially stronger correlation (0.15 to 0.24) between simulated and observed $BC_{snow}$ in the region (Table 6). WBF further reduces the average bias across the Arctic by 70%. Overall, modeled $BC_{snow}$ is poorly correlated with observations (r = 0.15 to 0.24) for all AeroCom models and GEOS-Chem. This disagreement is probably resulted from a common problem in the Arctic, which is the poorly constrained meteorological fields including precipitation in the Arctic due to the scarcity of observations in the region (Sect. 4.4). Our model results show that doubling (halving) precipitation introduces a much larger positive (negative) bias, similar as the magnitude of the overall effects of flaring emissions and the WBF effect (Sect. 4.4).

BC loading in the Arctic in this study exceeds the high end of the previous AeroCom estimates (0.02−0.34 mg $m^{-2}$) by including the WBF effect (Table 6). We find that BC scavenging efficiency play a more important role on determining BC loading in the Arctic than emissions, $v_d$, and precipitation. BC loading in this region increases by 13% from flaring emissions, which represents a ~70% enhancement to previous emission estimates, and by 7% from updated $v_d$, which in some cases are a factor of two to three larger. In addition, Arctic BC loading increases by 12% when precipitation is halved and decreases by 14% when precipitation is doubled. WBF reduces BC scavenging efficiency in mixed-phase clouds by 20−80% and increases annual BC loading by 70% in the Arctic. This large sensitivity of BC loading in the Arctic to treatments of BC scavenging efficiency in mixed-phase clouds and in ice clouds is also shown by previous studies. For example, Bourgeois and Bey (2011) reduced the scavenging efficiency in mixed-phase clouds from 0.10−0.75 to a uniform value of 0.06 in the ECHAM5-HAMMOZ model (Pozzoli et al., 2008) and found that the resulting $BC_{air}$ in the Arctic increased by up to a factor of ten and were in improved agreement with aircraft observations. In addition, their model results of BC burden in the Arctic were five times higher. We note here that a scavenging efficiency of 0.06 is on the low end of observed values in mixed-phase clouds (Cozic et al., 2007;

Verheggen et al., 2007), which leads to a considerably larger WBF effect. Liu et al. (2011) found that lowering BC scavenging efficiency in ice clouds (from 0.2 to 0.01) in AM3 model (Anderson et al., 2004) dramatically enhanced BC transport to the Arctic (nearly 10 times higher) and improved model comparison with aircraft observations. Browse et al. (2012) suppressed the scavenging of soluble BC in ice clouds in the GLOMAP model (Mann et al., 2010) and found that the resulting $BC_{air}$ in the Arctic were six times higher. Better characterization of scavenging efficiency in all could types globally is thus critical for accurately reproducing BC distribution and the associated climatic effects in the Arctic.

**6. Summary and conclusions**

This study sought to understand the capability of GEOS-Chem in simulating BC distribution both in air and in snow in the Arctic and the controlling factors. We evaluated the model simulation against $BC_{snow}$ measurements across the Arctic and in-situ measurements of surface $BC_{air}$ at Denali in low Arctic, Barrow, Alert and Zeppelin in high Arctic, and Summit in the free troposphere. We also examined the role of gas flaring emissions, $v_d$, the WBF effect, and precipitation on BC distribution in the Arctic. We first included BC emissions from a missing source in the current emission inventories–natural gas flares. We than implied resistance-in-series method to estimate $v_d$ of BC over snow and ice to replace the uniform constant $v_d$ of 0.03 cm $s^{-1}$ over snow and ice. We also parameterized the effects of WBF process on BC scavenging efficiency in mixed-phase clouds. WBF was stronger at lower temperature.

With all these improvements, the discrepancy of $BC_{snow}$ across the whole Arctic decreased substantially (from -40% to -10%). In the eight sub-regions, the simulated $BC_{snow}$ agreed with observations within a factor of two. We also found that including flaring emissions significantly improves the simulation of $BC_{snow}$ with a strong reduction of discrepancy (from -40% to -20%) and an increase of correlation coefficient with observations (from 0.15 to 0.24). WBF further reduced the discrepancy of $BC_{snow}$ to within -10%, with the largest improvement in the North American section in the Arctic. Simulation of $BC_{snow}$ with the abovementioned improvements was among the best AeroCom models evaluated by Jiao et al. (2014). The resulting $BC_{air}$ agreed with observations within a factor of 2, also among the best simulations in Eckhardt et al. (2015).

In addition to these physical processes, we also tested the sensitivity of $BC_{snow}$ to precipitation in the Arctic, which is poorly constrained due to the sparse observation network. The difference of precipitation rate in the region among GEOS-5, GPCP and CMAP was up to a factor of ten. Our model results suggested that the negative (positive) bias introduced by doubling (halving) precipitation rate in the Arctic was similar to the combined effects of flaring emissions and WBF. Although this effect might be exaggerated because our method of estimating $BC_{snow}$ strongly depends on precipitation flux, it is worthwhile to notice the importance of precipitation on $BC_{snow}$ simulation.

There remain large uncertainties in flaring emission factors, spatial and temporal variation of flaring emissions, dry deposition velocities of BC and BC scavenging efficiencies in clouds. Process-specific measurements, particularly in the Arctic, are useful to better constrain the simulation of BC distribution in the region. For example, we need direct measurements of emission factors of gas flares in the Western Extreme North of Russia, including their spatial and temporal variations. In addition, $v_d$ measurements specific to BC particles over snow and ice covered land surfaces should be made in winter. Measurements of BC scavenging efficiency in clouds, particularly in mixed-phase and ice clouds in the Arctic, are also needed to constrain BC wet deposition.

**Acknowledgements**

This study was funded by NASA grant NNX14AF11G from the Atmospheric Chemistry Modeling and Analysis Program (ACMAP). The authors thank Y. Kondo, J. P. Schwarz, S. G. Warren, and H. Liu for helpful discussions. We would also like to thank the Global Monitoring Division at NOAA Earth System Research Laboratory, the Atmospheric Science and Technology Directorate at Environment Canada and SFT Norway for providing data. The Swedish Environmental Protection Agency and the Swedish Research Council have sponsored BC measurements at Zeppelin. We would also like to thank 'Soot In Arctic Snow' group from University of Washington for providing measurements of BC concentration in snow in the Arctic. We thank the two reviewers for their valuable comments on this manuscript.

**References**

Allen, D. J., Kasibhatla, P., Thompson, A. M., Rood, R. B., Doddridge, B. G., Pickering, K. E., Hudson, R. D., and Lin, S. J.: Transport-induced interannual variability of carbon monoxide determined using a chemistry and transport model, J Geophys Res-Atmos, 101, 28655-28669, doi:10.1029/96jd02984, 1996a.

Allen, D. J., Rood, R. B., Thompson, A. M., and Hudson, R. D.: Three-dimensional radon 222 calculations using assimilated meteorological data and a convective mixing algorithm, J Geophys Res-Atmos, 101, 6871-6881, doi:10.1029/95jd03408, 1996b.

Anderson, J. L. e. a.: The New GFDL Global Atmosphere and Land Model AM2–LM2: Evaluation with Prescribed SST Simulations, Journal of Climate, 17, 4641-4673, doi:10.1175/jcli-3223.1, 2004.

Arakawa, A., and Schubert, W. H.: Interaction of a Cumulus Cloud Ensemble with the Large-Scale Environment, Part I, J Atmos Sci, 31, 674-701, doi:10.1175/1520-0469, 1974.

Barahona, D., Molod, A., Bacmeister, J., Nenes, A., Gettelman, A., Morrison, H., Phillips, V., and Eichmann, A.: Development of two-moment cloud microphysics for liquid and ice within the NASA Goddard Earth Observing System Model (GEOS-5), Geosci. Model Dev., 7, 1733-1766, doi:10.5194/gmd-7-1733-2014, 2014.

Barrie, L. A.: First International Conference on Atmospheric Sciences and Applications to Air Quality Arctic air pollution: An overview of current knowledge, Atmospheric Environment (1967), 20, 643-663, doi:10.1016/0004-6981(86)90180-0, 1986.

Bergeron, T.: On the physics of clouds and precipitation. Proces Verbaux de l'Association de Météorologie, Interna- tional Union of Geodesy and Geophysics, 156–178, 1935.

Bergin, M. H., Jaffrezo, J. L., Davidson, C. I., Dibb, J. E., Pandis, S. N., Hillamo, R., Maenhaut, W., Kuhns, H. D., and Makela, T.: The contributions of snow, fog, and dry deposition to the summer flux of anions and cations at Summit, Greenland, Journal of Geophysical Research: Atmospheres, 100, 16275-16288, doi:10.1029/95jd01267, 1995.

Bond, T. C., Anderson, T. L., and Campbell, D.: Calibration and Intercomparison of Filter-Based Measurements of Visible Light Absorption by Aerosols, Aerosol Science and Technology, 30, 582-600, doi:10.1080/027868299304435, 1999.

Bond, T. C., and Bergstrom, R. W.: Light Absorption by Carbonaceous Particles: An Investigative Review, Aerosol Science and Technology, 40, 27-67, doi:10.1080/02786820500421521, 2006.

Bond, T. C., Bhardwaj, E., Dong, R., Jogani, R., Jung, S., Roden, C., Streets, D. G., and Trautmann, N. M.: Historical emissions of black and organic carbon aerosol from energy-related combustion, 1850–2000, Global Biogeochemical Cycles, 21, GB2018, doi:10.1029/2006gb002840, 2007.

Bond, T. C., Doherty, S. J., Fahey, D. W., Forster, P. M., Berntsen, T., DeAngelo, B. J., Flanner, M. G., Ghan, S., Kärcher, B., Koch, D., Kinne, S., Kondo, Y., Quinn, P. K., Sarofim, M. C., Schultz, M. G., Schulz, M., Venkataraman, C., Zhang, H., Zhang, S., Bellouin, N., Guttikunda, S. K., Hopke, P. K., Jacobson, M. Z., Kaiser, J. W., Klimont, Z., Lohmann, U., Schwarz, J. P.,

Shindell, D., Storelvmo, T., Warren, S. G., and Zender, C. S.: Bounding the role of black carbon in the climate system: A scientific assessment, Journal of Geophysical Research: Atmospheres, 118, 5380-5552, doi:10.1002/jgrd.50171, 2013.

Bourgeois, Q., and Bey, I.: Pollution transport efficiency toward the Arctic: Sensitivity to aerosol scavenging and source regions, Journal of Geophysical Research: Atmospheres, 116, D08213, doi:10.1029/2010jd015096, 2011.

Bradbury, J., Clement, Z., and Down, A.: Greenhouse gas emissions and fuel use within the Natural gas supply chain - Sankey Diagram methodology, Office of Energy Policy and System Analysis, U.S. Department of Energy, 2015

Browse, J., Carslaw, K. S., Arnold, S. R., Pringle, K., and Boucher, O.: The scavenging processes controlling the seasonal cycle in Arctic sulphate and black carbon aerosol, Atmos Chem Phys, 12, 6775-6798, doi:10.5194/acp-12-6775-2012, 2012.

CAPP: A recommended approach to completing the national pollutant release inventory (NPRI) for the upstream oil and gas industry, Canadian Association of Petroleum Producers (CAPP), available from: http://www.capp.ca/library/publications/policyRegulatory/pages/pubInfo.aspx?DocId=119572, 2007.

Chen, Y., Li, Q., Randerson, J. T., Lyons, E. A., Kahn, R. A., Nelson, D. L., and Diner, D. J.: The sensitivity of CO and aerosol transport to the temporal and vertical distribution of North American boreal fire emissions, Atmos. Chem. Phys., 9, 6559-6580, doi:10.5194/acp-9-6559-2009, 2009.

Chow, J. C., Watson, J. G., Pritchett, L. C., Pierson, W. R., Frazier, C. A., and Purcell, R. G.: The dri thermal/optical reflectance carbon analysis system: description, evaluation and applications in U.S. Air quality studies, Atmospheric Environment. Part A. General Topics, 27, 1185-1201, doi:10.1016/0960-1686(93)90245-T, 1993.

Chow, J. C., Watson, J. G., Chen, L. W. A., Arnott, W. P., Moosmüller, H., and Fung, K.: Equivalence of Elemental Carbon by Thermal/Optical Reflectance and Transmittance with Different Temperature Protocols, Environmental Science & Technology, 38, 4414-4422, doi:10.1021/es034936u, 2004.

Clarke, A. D., and Noone, K. J.: Soot in the Arctic Snowpack - a Cause for Perturbations in Radiative-Transfer, Atmos Environ, 19, 2045-2053, doi:10.1016/0004-6981(85)90113-1, 1985.

Clarke, A. D., Noone, K. J., Heintzenberg, J., Warren, S. G., and Covert, D. S.: Aerosol light absorption measurement techniques: Analysis and intercomparisons, Atmospheric Environment (1967), 21, 1455-1465, doi:10.1016/0004-6981(67)90093-5, 1987.

Cozic, J., Verheggen, B., Mertes, S., Connolly, P., Bower, K., Petzold, A., Baltensperger, U., and Weingartner, E.: Scavenging of black carbon in mixed phase clouds at the high alpine site Jungfraujoch, Atmos. Chem. Phys., 7, 1797-1807, doi:10.5194/acp-7-1797-2007, 2007.

Delene, D. J., and Ogren, J. A.: Variability of Aerosol Optical Properties at Four North American Surface Monitoring Sites, J Atmos Sci, 59, 1135-1150, doi:10.1175/1520-0469, 2002.

Di Liberto, L., Angelini, F., Pietroni, I., Cairo, F., Di Donfrancesco, G., Viola, A., Argentini, S., Fierli, F., Gobbi, G., Maturilli, M., Neuber, R., and Snels, M.: Estimate of the Arctic Convective Boundary Layer Height from Lidar Observations: A Case Study, Advances in Meteorology, 2012, 9, doi:10.1155/2012/851927, 2012.

Doherty, S. J., Warren, S. G., Grenfell, T. C., Clarke, A. D., and Brandt, R. E.: Light-absorbing impurities in Arctic snow, Atmos Chem Phys, 10, 11647-11680, doi:10.5194/acp-10-11647-2010, 2010.

Doherty, S. J., Grenfell, T. C., Forsström, S., Hegg, D. L., Brandt, R. E., and Warren, S. G.: Observed vertical redistribution of black carbon and other insoluble light-absorbing particles in melting snow, Journal of Geophysical Research: Atmospheres, 118, 5553-5569, doi:10.1002/jgrd.50235, 2013.

Doherty, S. J., Bitz, C. M., and Flanner, M. G.: Biases in modeled surface snow BC mixing ratios in prescribed-aerosol climate model runs, Atmos Chem Phys, 14, 11697-11709, doi:10.5194/acp-14-11697-2014, 2014.

Dovland, H., and Eliassen, A.: Dry deposition on a snow surface, Atmospheric Environment (1967), 10, 783-785, doi:10.1016/0004-6981(76)90080-9, 1976.

Duan, B., Fairall, C. W., and Thomson, D. W.: Eddy Correlation Measurements of the Dry Deposition of Particles in Wintertime, Journal of Applied Meteorology, 27, 642-652, doi:10.1175/1520-0450, 1988.

Eckhardt, S., Quennehen, B., Olivié, D. J. L., Berntsen, T. K., Cherian, R., Christensen, J. H., Collins, W., Crepinsek, S., Daskalakis, N., Flanner, M., Herber, A., Heyes, C., Hodnebrog, Ø., Huang, L., Kanakidou, M., Klimont, Z., Langner, J., Law, K. S., Lund, M. T., Mahmood, R., Massling, A., Myriokefalitakis, S., Nielsen, I. E., Nøjgaard, J. K., Quaas, J., Quinn, P. K., Raut, J.-C., Rumbold, S. T., Schulz, M., Sharma, S., Skeie, R. B., Skov, H., Uttal, T., von Salzen, K., and Stohl, A.: Current model capabilities for simulating black carbon and sulfate concentrations in the Arctic atmosphere: a multi-model evaluation using a comprehensive measurement data set, Atmos. Chem. Phys., 15, 9413-9433, doi:10.5194/acp-15-9413-2015, 2015.

Eleftheriadis, K., Vratolis, S., and Nyeki, S.: Aerosol black carbon in the European Arctic: Measurements at Zeppelin station, Ny-Ålesund, Svalbard from 1998–2007, Geophysical Research Letters, 36, doi:10.1029/2008gl035741, 2009.

Elvidge, C. D., Ziskin, D., Baugh, K. E., Tuttle, B. T., Ghosh, T., Pack, D. W., Erwin, E. H., and Zhizhin, M.: A Fifteen Year Record of Global Natural Gas Flaring Derived from Satellite Data, Energies, 2, 595-622, doi:10.3390/en20300595, 2009.

Elvidge, C. D., Kimberly E.; Ziskin, Daniel; Anderson, Sharolyn; Ghosh, Tilottoma: Estimation of Gas Flaring Volumes Using NASA MODIS Fire Detection Products, 2011.

Elvidge, C. D., Zhizhin, M., Baugh, K., Hsu, F.-C., and Ghosh, T.: Methods for global survey of natural gas flaring from visible infrared imaging radiometer suite data, Energies, 9(1), 14, doi:10.3390/en9010014, 2016.

Fan, J., Ghan, S., Ovchinnikov, M., Liu, X., Rasch, P. J., and Korolev, A.: Representation of Arctic mixed-phase clouds and the Wegener-Bergeron-Findeisen process in climate models: Perspectives from a cloud-resolving study, Journal of Geophysical Research: Atmospheres, 116, doi:10.1029/2010jd015375, 2011.

Findeisen, W.: Kolloid-meteorologische Vorgänge bei Neiderschlags-bildung. Meteor. Z., 55, 121–133. 1938.

Fisher, J. A., Jacob, D. J., Wang, Q., Bahreini, R., Carouge, C. C., Cubison, M. J., Dibb, J. E., Diehl, T., Jimenez, J. L., Leibensperger, E. M., Lu, Z., Meinders, M. B. J., Pye, H. O. T., Quinn, P. K., Sharma, S., Streets, D. G., van Donkelaar, A., and Yantosca, R. M.: Sources, distribution, and acidity of sulfate–ammonium aerosol in the Arctic in winter–spring, Atmos Environ, 45, 7301-7318, doi:10.1016/j.atmosenv.2011.08.030, 2011.

Flanner, M. G., Zender, C. S., Randerson, J. T., and Rasch, P. J.: Present-day climate forcing and response from black carbon in snow, Journal of Geophysical Research, 112, doi:10.1029/2006jd008003, 2007.

Flanner, M. G., Zender, C. S., Hess, P. G., Mahowald, N. M., Painter, T. H., Ramanathan, V., and Rasch, P. J.: Springtime warming and reduced snow cover from carbonaceous particles, Atmos Chem Phys, 9, 2481-2497, 2009.

Flanner, M. G., Shell, K. M., Barlage, M., Perovich, D. K., and Tschudi, M. A.: Radiative forcing and albedo feedback from the Northern Hemisphere cryosphere between 1979 and 2008, Nature Geosci, 4, 151-155, 2011.

Flanner, M. G., Liu, X., Zhou, C., Penner, J. E., and Jiao, C.: Enhanced solar energy absorption by internally-mixed black carbon in snow grains, Atmos Chem Phys, 12, 4699-4721, doi:10.5194/acp-12-4699-2012, 2012.

Flanner, M. G.: Arctic climate sensitivity to local black carbon, Journal of Geophysical Research: Atmospheres, 118, 1840-1851, doi:10.1002/jgrd.50176, 2013.

Forsström, S., Isaksson, E., Skeie, R. B., Ström, J., Pedersen, C. A., Hudson, S. R., Berntsen, T. K., Lihavainen, H., Godtliebsen, F., and Gerland, S.: Elemental carbon measurements in European Arctic snow packs, Journal of Geophysical Research: Atmospheres, 118, 13,614-613,627, doi:10.1002/2013jd019886, 2013.

Fukuta, N., and Takahashi, T.: The Growth of Atmospheric Ice Crystals: A Summary of Findings in Vertical Supercooled Cloud Tunnel Studies, J Atmos Sci, 56, 1963-1979, doi:10.1175/1520-0469, 1999.

Gallagher, M. W.: Measurements and parameterizations of small aerosol deposition velocities to grassland, arable crops, and forest: Influence of surface roughness length on deposition, Journal of Geophysical Research, 107, doi:10.1029/2001jd000817, 2002.

Garrett, T. J., Zhao, C., and Novelli, P. C.: Assessing the relative contributions of transport efficiency and scavenging to seasonal variability in Arctic aerosol, Tellus B, 62, 190-196, doi:10.1111/j.1600-0889.2010.00453.x, 2010.

Garrett, T. J., Brattström, S., Sharma, S., Worthy, D. E. J., and Novelli, P.: The role of scavenging in the seasonal transport of black carbon and sulfate to the Arctic, Geophysical Research Letters, 38, doi:10.1029/2011gl048221, 2011.

Giorgi, F., and Chameides, W. L.: Rainout lifetimes of highly soluble aerosols and gases as inferred from simulations with a general circulation model, Journal of Geophysical Research: Atmospheres, 91, 14367-14376, doi:10.1029/JD091iD13p14367, 1986.

Goldenson, N., Doherty, S. J., Bitz, C. M., Holland, M. M., Light, B., and Conley, A. J.: Arctic climate response to forcing from light-absorbing particles in snow and sea ice in CESM, Atmos. Chem. Phys., 12, 7903-7920, doi:10.5194/acp-12-7903-2012, 2012.

Gronlund, A. N., Douglas; Koponen, Ismo K.; Virkkula, Aki; Hansson, Margareta E.: Aerosol dry deposition measured with eddy-covariance technique at Wasa and Aboa, Dronning Maud Land, Antarctica, Annals of Glaciology, 35, 7, 2002.

Hack, J. J.: Parameterization of moist convection in the National Center for Atmospheric Research community climate model (CCM2), J Geophys Res-Atmos, 99, 5551-5568, doi:10.1029/93jd03478, 1994.

Hagler G. S. W., Bergin, M. H., Smith, E. A., Dibb, J. E.: A summer time series of particulate carbon in the air and snow at Summit, Greenland, J. Geophys. Res., 112, D21309, doi:10.1029/2007JD008993, 2007.

Hallberg, A., Ogren, J. A., Noone, K. J., Heintzenberg, J., Berner, A., Solly, I., Kruisz, C., Reischl, G., Fuzzi, S., Facchini, M. C., Hansson, H. C., Wiedensohler, A., and Svenningsson, I. B.: Phase partitioning for different aerosol species in fog, Tellus B; Vol 44, No 5 (1992),

Hallberg, A., Noone, K. J., Ogren, J. A., Svenningsson, I. B., Flossmann, A., Wiedensohler, A., Hansson, H. C., Heintzenberg, J., Anderson, T. L., Arends, B. G., and Maser, R.: Phase Partitioning of Aerosol Particles in Clouds at Kleiner Feldberg, in: The Kleiner Feldberg Cloud Experiment 1990: EUROTRAC Subproject Ground-Based Cloud Experiment (GCE), edited by: Fuzzi, S., Springer Netherlands, Dordrecht, 107-127, 1995.

Hansen, J., and Nazarenko, L.: Soot climate forcing via snow and ice albedos, P Natl Acad Sci USA, 101, 423-428, doi:10.1073/pnas.2237157100, 2004.

He, C., Li, Q. B., Liou, K. N., Zhang, J., Qi, L., Mao, Y., Gao, M., Lu, Z., Streets, D. G., Zhang, Q., Sarin, M. M., and Ram, K.: A global 3-D CTM evaluation of black carbon in the Tibetan Plateau, Atmos. Chem. Phys., 14, 7091-7112, doi:10.5194/acp-14-7091-2014, 2014a.

He, C., Li, Q. B., Liou, K. N., Takano, Y., Gu, Y., Qi, L., Mao, Y. H., and Leung, L. R.: Black carbon radiative forcing over the Tibetan Plateau, Geophys. Res. Lett., 41, 7806-7813, doi:10.1002/2014gl062191, 2014b.

He, C., Li, Q., Liou, K.-N., Qi, L., Tao, S., and Schwarz, J. P.: Microphysics-based black carbon aging in a global CTM: constraints from HIPPO observations and implications for global black carbon budget, Atmos. Chem. Phys., 16, 3077-3098, doi:10.5194/acp-16-3077-2016, 2016.

Hegg, D. A., Clarke, A. D., Doherty, S. J., and StrÖM, J.: Measurements of black carbon aerosol washout ratio on Svalbard, Tellus B, 63, 891-900, doi:10.1111/j.1600-0889.2011.00577.x, 2011.

Held, A., Brooks, I. M., Leck, C., and Tjernström, M.: On the potential contribution of open lead particle emissions to the central Arctic aerosol concentration, Atmos Chem Phys, 11, 3093-3105, doi:10.5194/acp-11-3093-2011, 2011.

Henning, S., Bojinski, S., Diehl, K., Ghan, S., Nyeki, S., Weingartner, E., Wurzler, S., and Baltensperger, U.: Aerosol partitioning in natural mixed-phase clouds, Geophysical Research Letters, 31, doi:10.1029/2003gl019025, 2004.

Hillamo, R. E., Kerminen, V. M., Maenhaut, W., Jaffrezo, J. L., Balachandran, S., and Davidson, C. I.: Arctic air, snow and ice chemistrySize distributions of atmospheric trace elements at dye 3, Greenland — I. Distribution characteristics and dry deposition velocities, Atmospheric Environment. Part A. General Topics, 27, 2787-2802, doi:10.1016/0960-1686(93)90311-L, 1993.

Hirdman, D., Burkhart, J. F., Sodemann, H., Eckhardt, S., Jefferson, A., Quinn, P. K., Sharma, S., Ström, J., and Stohl, A.: Long-term trends of black carbon and sulphate aerosol in the Arctic: changes in atmospheric transport and source region emissions, Atmos. Chem. Phys., 10, 9351-9368, doi:10.5194/acp-10-9351-2010, 2010.

Hitzenberger, R., Berner, A., Kromp, R., Kasper-Giebl, A., Limbeck, A., Tscherwenka, W., and Puxbaum, H.: Black carbon and other species at a high-elevation European site (Mount Sonnblick, 3106 m, Austria): Concentrations and scavenging efficiencies, Journal of Geophysical Research: Atmospheres, 105, 24637-24645, doi:10.1029/2000jd900349, 2000.

Hitzenberger, R., Berner, A., Giebl, H., Drobesch, K., Kasper-Giebl, A., Loeflund, M., Urban, H., and Puxbaum, H.: Black carbon (BC) in alpine aerosols and cloud water—concentrations and scavenging efficiencies, Atmos Environ, 35, 5135-5141, doi:10.1016/S1352-2310(01)00312-0, 2001.

Huang, K., Fu, J. S., Prikhodko, V. Y., Storey, J. M., Romanov, A., Hodson, E. L., Cresko, J., Morozova, I., Ignatieva, Y., and Cabaniss, J.: Russian anthropogenic black carbon: Emission reconstruction and Arctic black carbon simulation, Journal of Geophysical Research: Atmospheres, 120, 11, 306-311, 333, doi:10.1002/2015jd023358, 2015.

Huang, L., Gong, S. L., Jia, C. Q., and Lavoué, D.: Importance of deposition processes in simulating the seasonality of the Arctic black carbon aerosol, Journal of Geophysical Research: Atmospheres, 115, doi:10.1029/2009jd013478, 2010.

Huffman, G. J., Adler, R. F., Morrissey, M. M., Bolvin, D. T., Curtis, S., Joyce, R., McGavock, B., and Susskind, J.: Global Precipitation at One-Degree Daily Resolution from Multisatellite Observations, Journal of Hydrometeorology, 2, 36-50, doi:10.1175/1525-7541, 2001.

IPCC: Climate Change 2014: Synthesis Report. Contribution of Working Groups I, II and III to the Fifth Assessment Report of the Intergovernmental Panel on Climate Change [Core Writing Team, R.K. Pachauri and L.A. Meyer (eds.)]. IPCC, Geneva, Switzerland, 151 pp, 2014

Jacobson, M. Z.: Climate response of fossil fuel and biofuel soot, accounting for soot's feedback to snow and sea ice albedo and emissivity, Journal of Geophysical Research: Atmospheres, 109, doi:10.1029/2004jd004945, 2004.

Jiao, C., Flanner, M. G., Balkanski, Y., Bauer, S. E., Bellouin, N., Berntsen, T. K., Bian, H., Carslaw, K. S., Chin, M., De Luca, N., Diehl, T., Ghan, S. J., Iversen, T., Kirkevåg, A., Koch, D., Liu, X., Mann, G. W., Penner, J. E., Pitari, G., Schulz, M., Seland, Ø., Skeie, R. B., Steenrod, S. D., Stier, P., Takemura, T., Tsigaridis, K., van Noije, T., Yun, Y., and Zhang, K.: An AeroCom assessment of black carbon in Arctic snow and sea ice, Atmos Chem Phys, 14, 2399-2417, doi:10.5194/acp-14-2399-2014, 2014.

Johnson, M. R., Devillers, R. W., and Thomson, K. A.: Quantitative Field Measurement of Soot Emission from a Large Gas Flare Using Sky-LOSA, Environmental Science & Technology, 45, 345-350, doi:10.1021/es102230y, 2011.

Keegan, K. M., Albert, M. R., McConnell, J. R., and Baker, I.: Climate change and forest fires synergistically drive widespread melt events of the Greenland Ice Sheet, Proceedings of the National Academy of Sciences, 111, 7964-7967, 2014.

Koch, D., Menon, S., Del Genio, A., Ruedy, R., Alienov, I., and Schmidt, G. A.: Distinguishing Aerosol Impacts on Climate over the Past Century, Journal of Climate, 22, 2659-2677, doi:10.1175/2008jcli2573.1, 2009.

Kopacz, M., Mauzerall, D. L., Wang, J., Leibensperger, E. M., Henze, D. K., and Singh, K.: Origin and radiative forcing of black carbon transported to the Himalayas and Tibetan Plateau, Atmos. Chem. Phys., 11, 2837-2852, doi:10.5194/acp-11-2837-2011, 2011.

Ladd, M. J., and Gajewski, K.: The North American summer Arctic front during 1948–2007, International Journal of Climatology, 30, 874-883, doi:10.1002/joc.1940, 2010.

Li, J. L. F., Waliser, D. E., Chen, W. T., Guan, B., Kubar, T., Stephens, G., Ma, H. Y., Deng, M., Donner, L., Seman, C., and Horowitz, L.: An observationally based evaluation of cloud ice water in CMIP3 and CMIP5 GCMs and contemporary reanalyses using contemporary satellite data, Journal of Geophysical Research: Atmospheres, 117, doi:10.1029/2012jd017640, 2012.

Lin, S. J., and Rood, R. B.: Multidimensional flux-form semi-Lagrangian transport schemes, Mon Weather Rev, 124, 2046-2070, doi:10.1175/1520-0493, 1996.

Liou, K. N., Takano, Y., He, C., Yang, P., Leung, L. R., Gu, Y., and Lee, W. L.: Stochastic parameterization for light absorption by internally mixed BC/dust in snow grains for application to climate models, J. Geophys. Res.-Atmos., 119, 7616-7632, doi:10.1002/2014jd021665, 2014.

Liston, G. E., and Sturm, M.: The role of winter sublimation in the Arctic moisture budget, Hydrology Research, 35, 325-334, 2004.

Liu, H., Jacob, D. J., Bey, I., and Yantosca, R. M.: Constraints from 210Pb and 7Be on wet deposition and transport in a global three-dimensional chemical tracer model driven by assimilated meteorological fields, Journal of Geophysical Research: Atmospheres, 106, 12109-12128, doi:10.1029/2000jd900839, 2001.

Liu, J., Fan, S., Horowitz, L. W., and Levy, H.: Evaluation of factors controlling long-range transport of black carbon to the Arctic, Journal of Geophysical Research, 116, doi:10.1029/2010jd015145, 2011.

Malm, W. C., Sisler, J. F., Huffman, D., Eldred, R. A., and Cahill, T. A.: Spatial and seasonal trends in particle concentration and optical extinction in the United States, Journal of Geophysical Research: Atmospheres, 99, 1347-1370, doi:10.1029/93jd02916, 1994.

Mann, G. W., Carslaw, K. S., Spracklen, D. V., Ridley, D. A., Manktelow, P. T., Chipperfield, M. P., Pickering, S. J., and Johnson, C. E.: Description and evaluation of GLOMAP-mode: a modal global aerosol microphysics model for the UKCA composition-climate model, Geosci. Model Dev., 3, 519-551, doi:10.5194/gmd-3-519-2010, 2010.

Marks, A. A., and King, M. D.: The effects of additional black carbon on the albedo of Arctic sea ice: variation with sea ice type and snow cover, The Cryosphere, 7, 1193-1204, 10.5194/tc-7-1193-2013, 2013.

McEwen, J. D. N., and Johnson, M. R.: Black carbon particulate matter emission factors for buoyancy-driven associated gas flares, Journal of the Air & Waste Management Association, 62, 307-321, doi:10.1080/10473289.2011.650040, 2012.

McNaughton, C. S., Clarke, A. D., Freitag, S., Kapustin, V. N., Kondo, Y., Moteki, N., Sahu, L., Takegawa, N., Schwarz, J. P., Spackman, J. R., Watts, L., Diskin, G., Podolske, J., Holloway, J. S., Wisthaler, A., Mikoviny, T., de Gouw, J., Warneke, C., Jimenez, J., Cubison, M., Howell, S. G., Middlebrook, A., Bahreini, R., Anderson, B. E., Winstead, E., Thornhill, K. L., Lack, D., Cozic, J., and Brock, C. A.: Absorbing aerosol in the troposphere of the Western Arctic during the 2008 ARCTAS/ARCPAC airborne field campaigns, Atmos. Chem. Phys., 11, 7561-7582, doi:10.5194/acp-11-7561-2011, 2011.

Moorthi, S., and Suarez, M. J.: Relaxed Arakawa-Schubert - a Parameterization of Moist Convection for General-Circulation Models, Mon Weather Rev, 120, 978-1002, doi: 10.1175/1520-0493, 1992.

Namazi, M., von Salzen, K., and Cole, J. N. S.: Simulation of black carbon in snow and its climate impact in the Canadian Global Climate Model, Atmos. Chem. Phys., 15, 10887-10904, doi:10.5194/acp-15-10887-2015, 2015.

Nilsson, E. D., and Rannik, Ü.: Turbulent aerosol fluxes over the Arctic Ocean: 1. Dry deposition over sea and pack ice, Journal of Geophysical Research: Atmospheres, 106, 32125-32137, doi:10.1029/2000jd900605, 2001.

Overland, J. E., and Turet, P.: Variability of the atmospheric energy flux across 708N computed from the GFDL data set. The Polar Oceans and Their Role in Shaping the Global Environ- ment, Geophys. Monogr., No. 84, Amer. Geophys. Union, 313–325, 1994.

WCRP: Proceedings of the Workshop on the Implementation of the Arctic Precipitation Data Archive (APDA) at the Global Precipitation Climatology Centre (GPCC), Offenbach, Germany, 10–12 July, 1996, Arctic Climate System Study, World Climate Research Programme. WCRP-98, WMO/TD 804, 127 pp. plus appendices, 2007. [Available from World Climate Research Programme, 7 bis, Avenue de la Paix, Case Postale 2300, CH-1211 Geneva 2, Switzerland.]

Park, R. J., Jacob, D. J., Chin, M., and Martin, R. V.: Sources of carbonaceous aerosols over the United States and implications for natural visibility, J Geophys Res-Atmos, 108, doi:10.1029/2002jd003190, 2003.

Park, R. J., Jacob, D. J., Palmer, P. I., Clarke, A. D., Weber, R. J., Zondlo, M. A., Eisele, F. L., Bandy, A. R., Thornton, D. C., Sachse, G. W., and Bond, T. C.: Export efficiency of black carbon aerosol in continental outflow: Global implications, J Geophys Res-Atmos, 110, doi:10.1029/2004jd005432, 2005.

Petzold, A., Ogren, J. A., Fiebig, M., Laj, P., Li, S. M., Baltensperger, U., Holzer-Popp, T., Kinne, S., Pappalardo, G., Sugimoto, N., Wehrli, C., Wiedensohler, A., and Zhang, X. Y.: Recommendations for reporting "black carbon" measurements, Atmos. Chem. Phys., 13, 8365-8379, doi:10.5194/acp-13-8365-2013, 2013.

Pozzoli, L., Bey, I., Rast, S., Schultz, M. G., Stier, P., and Feichter, J.: Trace gas and aerosol interactions in the fully coupled model of aerosol-chemistry-climate ECHAM5-HAMMOZ: 1. Model description and insights from the spring 2001 TRACE-P experiment, Journal of Geophysical Research: Atmospheres, 113, doi:10.1029/2007jd009007, 2008.

Qi, L., Li, Q.B., He, C., Wang, X., and Huang, J.P.: Effects of Wegener-Bergeron-Findeisen Process on Global Black Carbon Distribution, Atmos. Chem. Phys., submitted, 2016

Quinn, P., Bates, T., Baum, E., Doubleday, N., Fiore, A., Flanner, M., Fridlind, A., Garrett, T. J., Koch, D., and Menon, S.: Short-lived pollutants in the Arctic: their climate impact and possible mitigation strategies, Atmospheric Chemistry and Physics, 8, 1723-1735, 2008.

Randerson, J. T., Chen, Y., van der Werf, G. R., Rogers, B. M., and Morton, D. C.: Global burned area and biomass burning emissions from small fires, Journal of Geophysical Research: Biogeosciences, 117, doi:10.1029/2012jg002128, 2012.

Schwarz, J. P., Holloway, J. S., Katich, J. M., McKeen, S., Kort, E. A., Smith, M. L., Ryerson, T. B., Sweeney, C., and Peischl, J.: Black Carbon Emissions from the Bakken Oil and Gas Development Region, Environmental Science & Technology Letters, 2, 281-285, doi:10.1021/acs.estlett.5b00225, 2015.

Schutgens, N. A. J., Gryspeerdt, E., Weigum, N., Tsyro, S., Goto, D., Schulz, M., and Stier, P.: Will a perfect model agree with perfect observations? The impact of spatial sampling, Atmos. Chem. Phys., 16, 6335-6353, doi:10.5194/acp-16-6335-2016, 2016.

Sellegri, K., Laj, P., Dupuy, R., Legrand, M., Preunkert, S., and Putaud, J. P.: Size-dependent scavenging efficiencies of multicomponent atmospheric aerosols in clouds, Journal of Geophysical Research: Atmospheres, 108, doi:10.1029/2002jd002749, 2003.

Serreze, M. C., Barry, R. G., and Walsh, J. E.: Atmospheric Water Vapor Characteristics at 70°N, Journal of Climate, 8, 719-731, doi:10.1175/1520-0442, 1995.

Serreze, M. C., and Hurst, C. M.: Representation of Mean Arctic Precipitation from NCEP–NCAR and ERA Reanalyses, Journal of Climate, 13, 182-201, doi:10.1175/1520-0442, 2000.

Sharma, S., Lavoué, D., Cachier, H., Barrie, L. A., and Gong, S. L.: Long-term trends of the black carbon concentrations in the Canadian Arctic, Journal of Geophysical Research: Atmospheres, 109, doi:10.1029/2003jd004331, 2004.

Sharma, S., Andrews, E., Barrie, L. A., Ogren, J. A., and Lavoué, D.: Variations and sources of the equivalent black carbon in the high Arctic revealed by long-term observations at Alert and Barrow: 1989–2003, Journal of Geophysical Research: Atmospheres, 111, doi:10.1029/2005jd006581, 2006.

Sharma, S., Ishizawa, M., Chan, D., Lavoué, D., Andrews, E., Eleftheriadis, K., and Maksyutov, S.: 16-year simulation of Arctic black carbon: Transport, source contribution, and sensitivity analysis on deposition, Journal of Geophysical Research: Atmospheres, 118, 943-964, doi:10.1029/2012jd017774, 2013.

Shindell, D., and Faluvegi, G.: Climate response to regional radiative forcing during the twentieth century, Nature Geosci, 2, 294-300, 2009.

Slowik, J. G., Cross, E. S., Han, J.-H., Davidovits, P., Onasch, T. B., Jayne, J. T., Williams, L. R., Canagaratna, M. R., Worsnop, D. R., Chakrabarty, R. K., Moosmüller, H., Arnott, W. P., Schwarz, J. P., Gao, R.-S., Fahey, D. W., Kok, G. L., and Petzold, A.: An Inter-Comparison of Instruments Measuring Black Carbon Content of Soot Particles, Aerosol Science and Technology, 41, 295-314, doi:10.1080/02786820701197078, 2007.

Stier, P., Feichter, J., Kinne, S., Kloster, S., Vignati, E., Wilson, J., Ganzeveld, L., Tegen, I., Werner, M., Balkanski, Y., Schulz, M., Boucher, O., Minikin, A., and Petzold, A.: The aerosol-climate model ECHAM5-HAM, Atmos. Chem. Phys., 5, 1125-1156, doi:10.5194/acp-5-1125-2005, 2005.

Stohl, A.: Characteristics of atmospheric transport into the Arctic troposphere, Journal of Geophysical Research: Atmospheres, 111, doi:10.1029/2005jd006888, 2006.

Stohl, A., Klimont, Z., Eckhardt, S., Kupiainen, K., Shevchenko, V. P., Kopeikin, V. M., and Novigatsky, A. N.: Black carbon in the Arctic: the underestimated role of gas flaring and residential combustion emissions, Atmos Chem Phys, 13, 8833-8855, doi:10.5194/acp-13-8833-2013, 2013.

Stroeve, J. C., Serreze, M. C., Holland, M. M., Kay, J. E., Malanik, J., and Barrett, A. P.: The Arctic's rapidly shrinking sea ice cover: a research synthesis, Climatic Change, 110, 1005-1027, doi:10.1007/s10584-011-0101-1, 2012.

Tedesco, M., Doherty, S., Fettweis, X., Alexander, P., Jeyaratnam, J., and Stroeve, J.: The darkening of the Greenland ice sheet: trends, drivers, and projections (1981–2100), The Cryosphere, 10, 477-496, doi:10.5194/tc-10-477-2016, 2016.

Textor, C., Schulz, M., Guibert, S., Kinne, S., Balkanski, Y., Bauer, S., Berntsen, T., Berglen, T., Boucher, O., Chin, M., Dentener, F., Diehl, T., Easter, R., Feichter, H., Fillmore, D., Ghan, S., Ginoux, P., Gong, S., Grini, A., Hendricks, J., Horowitz, L., Huang, P., Isaksen, I., Iversen, I., Kloster, S., Koch, D., Kirkevåg, A., Kristjansson, J. E., Krol, M., Lauer, A., Lamarque, J. F., Liu, X., Montanaro, V., Myhre, G., Penner, J., Pitari, G., Reddy, S., Seland, Ø., Stier, P., Takemura, T., and Tie, X.: Analysis and quantification of the diversities of aerosol life cycles within AeroCom, Atmos. Chem. Phys., 6, 1777-1813, doi:10.5194/acp-6-1777-2006, 2006.

Textor, C., Schulz, M., Guibert, S., Kinne, S., Balkanski, Y., Bauer, S., Berntsen, T., Berglen, T., Boucher, O., Chin, M., Dentener, F., Diehl, T., Feichter, J., Fillmore, D., Ginoux, P., Gong, S., Grini, A., Hendricks, J., Horowitz, L., Huang, P., Isaksen, I. S. A., Iversen, T., Kloster, S., Koch, D., Kirkevåg, A., Kristjansson, J. E., Krol, M., Lauer, A., Lamarque, J. F., Liu, X., Montanaro, V., Myhre, G., Penner, J. E., Pitari, G., Reddy, M. S., Seland, Ø., Stier, P., Takemura, T., and Tie, X.: The effect of harmonized emissions on aerosol properties in global models – an AeroCom experiment, Atmos. Chem. Phys., 7, 4489-4501, doi:10.5194/acp-7-4489-2007, 2007.

US EPA: Compilation of air pollutant emission factors - volume I: stationary point and area sources, AP-42 5th Edition, US Environmental Protection Agency (US EPA), Springfield, VA, 1995.

van der Werf, G. R., Randerson, J. T., Giglio, L., Collatz, G. J., Mu, M., Kasibhatla, P. S., Morton, D. C., DeFries, R. S., Jin, Y., and van Leeuwen, T. T.: Global fire emissions and the contribution of deforestation, savanna, forest, agricultural, and peat fires (1997–2009), Atmos. Chem. Phys., 10, 11707-11735, doi:10.5194/acp-10-11707-2010, 2010.

Verheggen, B., Cozic, J., Weingartner, E., Bower, K., Mertes, S., Connolly, P., Gallagher, M., Flynn, M., Choularton, T., and Baltensperger, U.: Aerosol partitioning between the interstitial and the condensed phase in mixed-phase clouds, Journal of Geophysical Research: Atmospheres, 112, doi:10.1029/2007jd008714, 2007.

Virkkula, A., Ahlquist, N. C., Covert, D. S., Arnott, W. P., Sheridan, P. J., Quinn, P. K., and Coffman, D. J.: Modification, Calibration and a Field Test of an Instrument for Measuring Light Absorption by Particles, Aerosol Science and Technology, 39, 68-83, doi:10.1080/027868290901963, 2005.

von Schneidemesser, E., Schauer, J. J., Hagler, G. S. W., and Bergin, M. H.: Concentrations and sources of carbonaceous aerosol in the atmosphere of Summit, Greenland, Atmos Environ, 43, 4155-4162, doi:10.1016/j.atmosenv.2009.05.043, 2009.

Wang, Q., Jacob, D. J., Fisher, J. A., Mao, J., Leibensperger, E. M., Carouge, C. C., Le Sager, P., Kondo, Y., Jimenez, J. L., Cubison, M. J., and Doherty, S. J.: Sources of carbonaceous aerosols and deposited black carbon in the Arctic in winter-spring: implications for radiative forcing, Atmos Chem Phys, 11, 12453-12473, doi:10.5194/acp-11-12453-2011, 2011.

Wang, Z. W., Gallet, J. C., Pedersen, C. A., Zhang, X. S., Ström, J., and Ci, Z. J.: Elemental carbon in snow at Changbai Mountain, northeastern China: concentrations, scavenging ratios, and dry deposition velocities, Atmos Chem Phys, 14, 629-640, doi:10.5194/acp-14-629-2014, 2014.

Warren, S. G.: Optical properties of snow, Reviews of Geophysics, 20, 67-89, doi:10.1029/RG020i001p00067, 1982.

Warren, S. G., and Wiscombe, W. J.: Dirty Snow after Nuclear-War, Nature, 313, 467-470, doi: 10.1038/313467a0, 1985.

Warren, S. G., Rigor, I. G., Untersteiner, N., Radionov, V. F., Bryazgin, N. N., Aleksandrov, Y. I., and Colony, R.: Snow Depth on Arctic Sea Ice, Journal of Climate, 12, 1814-1829, doi:10.1175/1520-0442, 1999.

Weingartner, E., Saathoff, H., Schnaiter, M., Streit, N., Bitnar, B., and Baltensperger, U.: Absorption of light by soot particles: determination of the absorption coefficient by means of aethalometers, Journal of Aerosol Science, 34, 1445-1463, doi:10.1016/S0021-8502(03)00359-8, 2003.

Wegener, A.: Thermodynamik der Atmosphäre. Leipzig, 331 pp, 1911.

Wesely, M. L., and Hicks, B. B.: Dry deposition and emission of small particles at the surface of the earth, 510-513, 1979.

Wesely, M. L.: Parameterization of surface resistances to gaseous dry deposition in regional-scale numerical models, Atmospheric Environment (1967), 23, 1293-1304, doi:10.1016/0004-6981(89)90153-4, 1989.

Weyant, C. L., Shepson, P. B., Subramanian, R., Cambaliza, M. O. L., Heimburger, A., McCabe, D., Baum, E., Stirm, B. H., and Bond, T. C.: Black Carbon Emissions from Associated Natural Gas Flaring, Environmental Science & Technology, 50, 2075-2081, doi:10.1021/acs.est.5b04712, 2016.

Wieringa, J.: Representativeness of Wind Observations at Airports, Bulletin of the American Meteorological Society, 61, 962-971, doi:10.1175/15200477, 1980.

Xie, P., and Arkin, P. A.: Global Precipitation: A 17-Year Monthly Analysis Based on Gauge Observations, Satellite Estimates, and Numerical Model Outputs, Bulletin of the American Meteorological Society, 78, 2539-2558, doi:10.1175/1520-0477, 1997.

Zhang, L., Gong, S., Padro, J., and Barrie, L.: A size-segregated particle dry deposition scheme for an atmospheric aerosol module, Atmos Environ, 35, 549-560, doi:10.1016/S1352-2310(00)00326-5, 2001.

Zhang, Q., Streets, D. G., Carmichael, G. R., He, K. B., Huo, H., Kannari, A., Klimont, Z., Park, I. S., Reddy, S., Fu, J. S., Chen, D., Duan, L., Lei, Y., Wang, L. T., and Yao, Z. L.: Asian emissions in 2006 for the NASA INTEX-B mission, Atmos. Chem. Phys., 9, 5131-5153, doi:10.5194/acp-9-5131-2009, 2009.

**Table 1: Measurements of BC in surface air in the Arctic.**

| Station | Temporal frequency | Data availability* | References |
|---|---|---|---|
| **Denali** (63.7°N, 149.0°W, 0.66 km) | 24-h average every 3 days | 91% | Malm *et al.* (1994) |
| **Barrow** (71.3°N, 156.6°W, 0.01 km) | 1 h | 46% | Bodhaine (1989) |
| **Alert** (82.3°N, 62.3°W, 0.21 km) | 1 h | 84% | Sharma *et al.* (2004) |
| **Zeppelin** (79°N, 12°E, 0.47 km) | 30 min | 79% | Eleftheriadis *et al.* (2009) |
| **Summit** (72.6°N, 38.5°W, 3.22 km) | 5 min | 95% | Delene and Ogren (2002) |

* ratio of available to total data (including available and missing data)

**Table 2: GEOS-Chem simulations of BC in the Arctic.**

| Experiments | | A | B | C | D |
|---|---|---|---|---|---|
| Anthropogenic emissions | Arctic | Bond *et al.* (2007) | Bond *et al.* (2007) and flaring emissions from Stohl *et al.* (2013) | | |
| | Asia | Zhang *et al.* (2009) | | | |
| | Rest of world | Bond *et al*. (2007) | | | |
| Biomass burning | | GFEDv3 (van der Werf *et al*., 2010), with updates from Randerson *et al.* (2012) | | | |
| BC aging | | e-folding time 1.15 days | | | |
| Deposition | Dry | 0.03 cm $s^{-1}$ over snow/ice and resistance-in-series over other surfaces (Wang *et al.*, 2011) | | Resistance-in-series over all surfaces (Wesely, 1989; Zhang *et al.*, 2001) | |
| | Wet | Liu *et al.* (2001) with updates from Wang *et al.* (2011) | | | |
| | | Riming: scavenging efficiency for hydrophilic BC is 100% in warm and mixed phase clouds | | | Account for both riming and WBF in mixed phase clouds (Fukuta *et al*., 1999; Verheggen *et al*., 2007; Cozic *et al*., 2007) |

**Table 3: Observed and simulated dry deposition velocity ($v_d$) using resistance-in-series method over snow and ice.**

| Region | Sample | Observed $v_d$ (cm $s^{-1}$) | Simulated $v_d$ (cm $s^{-1}$) | References | Particle diameter |
|---|---|---|---|---|---|
| Arctic Ocean | Open water leads, ice ridges, snow and ice surfaces | 0.027-0.068[a] | 0.006-0.070[a] | Held *et al.* (2011) | < 50 nm |
| Arctic Ocean | Open sea | 0.19[b] | | Nilsson and Rannik (2001) | |
| Arctic Ocean | Frozen, partly snow-covered ice | 0.03[b] | 0.013-0.22[b] | Nilsson and Rannik (2001) | Mostly ultrafine and Aitken mode |
| Arctic Ocean | Summer lead | 0.034[b] | | Nilsson and Rannik (2001) | |
| Arctic Ocean | Freeze-up lead | 0.091[b] | | Nilsson and Rannik (2001) | |
| Greenland | Snow (sulfate) | 0.023-0.062[c] | 0.007-0.16[c] | Bergin *et al.* (1995) | < 10 μm |
| Greenland | Snow (sulfate) | 0.01-0.18[d] | 0.007-0.20[d] | Hillamo *et al.* (1993) | 0.6 μm |
| Greenland | Snow | 0.2-0.7 | | Hillamo *et al.* (1993) | 2 μm |
| Antarctic | Snow grass | 0.02-0.1 | | Wesely *et al.* (1979) | 0.05-1.0 μm |
| Antarctic | Smooth snow surface | 0.33 (0.08-1.89) | | Grönlund *et al.* (2002) | 14 nm |
| Antarctic | Rocky surface interrupted by snow | 0.8 (0.2-2.4) | | Grönlund *et al.* (2002) | 42 nm |
| Norway | Snow | 0.06-0.38 | | Dovland and Elliassen (1976) | |
| Pennsylvania | Snow covered farm land in December | 0.034±0.014 | | Duan *et al.* (1988) | 0.15-0.3 μm |
| Mt. Changbai | Snow covered mountain (BC) | 0.16-1.52[e] | 0.09-0.14[e] | Wang *et al.* (2014) | |

[a] This range of measurements are medians of dry deposition velocities derived from aerosol number fluxes measured by an eddy covariance system over different surface types (open water leads, ice ridges, snow and ice surfaces) in the Arctic Ocean between 2°−10° W longitude and 87°−87.5° N latitude in late August 2008 (Held et al., 2011). The simulated dry deposition velocities are sampled at the same region during the same time period as observations for BC particles.

[b] Observations are medians of dry deposition velocities derived from aerosol number fluxes measured by an eddy covariance system over different surface types in late July and early August in 1996 in the Arctic Ocean for ultra fine and Aitken mode aerosol particles (Nilsson and Rannik, 2001). Simulations are sampled in the same region during the same months as observations in 2008 for BC particles.

[c] Sulpate dry deposition velocities were derived based on particle mass using surrogate surfaces and impactor data at site Summit, Greenland in July 1993 (Bergin et al., 1995). Simulations are sampled at the same site during July 2008 for BC particles.

[d] Sulpate dry deposition velocities were derived based on particle mass from Cascade impactor at Dye 3 on the south-central Greenland Ice Sheet in March 1989 (Hillamo et al., 1993). Simulations are sampled at the same site during March 2008 for BC particles.

e The dry deposition velocities specific to BC particles were derived from measured surface enhancement of BC in snow between two snow events at Changbai Mountain in Northern China in winter (December, January, and February) in 2009-2012 (Wang et al., 2014). Simulations are sampled at the same site during the same time period for BC particles.

**Table 4: Observed and GEOS-Chem simulated BC concentration in snow in the Arctic (ng $g^{-1}$, see Fig. 1).**

| | | | Arctic | Alaska | Arctic Ocean | Canadian Sub-Arctic | Canadian Arctic | Greenland | Ny_Ålesund | Russia | Tromsø |
|---|---|---|---|---|---|---|---|---|---|---|---|
| **Sample size** | | | 334 | 3 | 23 | 34 | 86 | 8 | 39 | 118 | 23 |
| **Arithmetic mean** | **Obs.** | | 19.8 | 12.4 | 8.0 | 14.8 | 8.8 | 3.2 | 13.7 | 28.3 | 19.3 |
| | **Experiment** | **A** | 10.9 (0.6[+]) | 6.0 (0.5) | 8.5 (1.1) | 7.7 (0.5) | 5.7 (0.7) | 3.6 (1.1) | 10.9 (0.8) | 12.3 (0.4) | 35.6 (1.8) |
| | | **B** | 15.0 (0.8) | 7.7 (0.6) | 10.8 (1.4) | 9.3 (0.6) | 6.7 (0.8) | 3.6 (1.1) | 14.9 (1.1) | 19.6 (0.7) | 41.8 (2.2) |
| | | **C** | 15.1 (0.8) | 8.0 (0.6) | 10.3 (1.3) | 9.1 (0.6) | 7.0 (0.8) | 4.3 (1.3) | 12.8 (0.9) | 20.7 (0.7) | 38.4 (2.0) |
| | | **D** | 16.0 (0.8) | 12.2 (1.0) | 12.4 (1.6) | 8.5 (0.6) | 8.8 (1.0) | 5.1 (1.6) | 14.9 (1.1) | 19.4 (0.7) | 45.8 (2.4) |
| **Geometric Mean** | **Obs.** | | 12.9 | 11.4 | 6.8 | 13.2 | 8.2 | 2.7 | 11.2 | 21.2 | 18.8 |
| | **Experiment** | **A** | 7.6 (0.6) | 5.9 (0.5) | 7.3 (1.1) | 5.9 (0.5) | 4.9 (0.6) | 2.3 (0.9) | 8.4 (0.8) | 9.3 (0.4) | 28.3 (1.5) |
| | | **B** | 10.4 (0.8) | 7.6 (0.7) | 9.6 (1.4) | 7.6 (0.6) | 6.1 (0.7) | 2.4 (0.9) | 11.4 (1.0) | 14.3 (0.7) | 35.1 (1.9) |
| | | **C** | 10.1 (0.8) | 7.9 (0.7) | 9.3 (1.4) | 7.3 (0.6) | 6.3 (0.8) | 2.8 (1.0) | 9.7 (0.9) | 13.9 (0.7) | 31.6 (1.7) |
| | | **D** | 11.5 (0.9) | 11.6 (1.0) | 11.6 (1.7) | 7.6 (0.6) | 8.1 (1.0) | 3.8 (1.4) | 11.9 (1.0) | 14.2 (0.7) | 37.2 (2.0) |
| **Median** | **Obs.** | | 11.8 | 11.0 | 7.6 | 12.8 | 8.9 | 2.5 | 11.9 | 22.1 | 19.1 |
| | **Experiment** | **A** | 6.9 (0.6) | 6.3 (0.6) | 6.4 (0.8) | 5.5 (0.4) | 4.1 (0.5) | 2.3 (0.9) | 8.4 (0.7) | 10.8 (0.5) | 25.2 (1.3) |
| | | **B** | 9.5 (0.8) | 7.6 (0.7) | 7.7 (1.0) | 7.3 (0.6) | 5.7 (0.6) | 2.3 (0.9) | 11.1 (0.9) | 16.1 (0.7) | 33.7 (1.8) |
| | | **C** | 8.7 (0.7) | 7.8 (0.7) | 8.5 (1.1) | 7.3 (0.6) | 6.0 (0.7) | 3.2 (1.3) | 9.2 (0.8) | 16.1 (0.7) | 29.2 (1.5) |
| | | **D** | 11.0 (0.9) | 12.1 (1.1) | 10.9 (1.4) | 6.8 (0.5) | 8.6 (1.0) | 5.7 (2.3) | 11.3 (1.0) | 16.9 (0.8) | 38.2 (2.0) |

[+]Ratio of model to observation

**Table 5: GEOS-Chem simulated BC dry deposition velocity (cm $s^{-1}$), dry deposition flux (ng $m^{-2}$ $d^{-1}$) and fraction of dry to total deposition (%) in the Arctic.**

| Region | Dry deposition velocity (cm $s^{-1}$) | | Dry deposition flux (ng $m^{-2}$ $d^{-1}$) | | | Total deposition flux (ng $m^{-2}$ $d^{-1}$) | | | Dry deposition fraction (%) | | |
|---|---|---|---|---|---|---|---|---|---|---|---|
| | Exp. B | Exps. C & D | Exp. B | Exp. C | Exp. D | Exp. B | Exp. C | Exp. D | Exp. B | Exp. C | Exp. D |
| **Alaska** | 0.03 | 0.08 | 787 | 1018 | 1906 | 2393 | 2469 | 3665 | 33 | 41 | 52 |
| **Arctic Ocean** | 0.03 | 0.07 | 662 | 789 | 1520 | 4480 | 4227 | 4733 | 15 | 19 | 32 |
| **Canadian sub-Arctic** | 0.04 | 0.08 | 841 | 1192 | 2297 | 5669 | 5596 | 5013 | 15 | 21 | 46 |
| **Canadian Arctic** | 0.03 | 0.07 | 661 | 988 | 1948 | 3194 | 3289 | 3343 | 20 | 30 | 58 |
| **Greenland** | 0.03 | 0.10 | 262 | 772 | 1804 | 3887 | 4245 | 4481 | 7 | 18 | 40 |
| **Ny_Ålesund** | 0.12 | 0.14 | 2654 | 2322 | 4861 | 19528 | 16713 | 19536 | 14 | 14 | 25 |
| **Russia** | 0.03 | 0.08 | 3092 | 5782 | 7288 | 13647 | 14465 | 12336 | 23 | 40 | 59 |
| **Tromsø** | 0.12 | 0.13 | 5826 | 5110 | 9339 | 46382 | 42085 | 49598 | 13 | 12 | 19 |

**Table 6: Model simulations of BC in the Arctic (60°N to 90°N).**

| | Model | Global Emission[b] (Tg yr$^{-1}$) | Arctic Emission[b] (Tg yr$^{-1}$) | Arctic Deposition[b] (Tg yr$^{-1}$) | Arctic Loading[c] (mg m$^{-2}$) | Arctic Lifetime[d] (d) | $BC_{snow}$ Bias[e] (ng g$^{-1}$) | $BC_{snow}$ $r$ [e] | Year of deposition field[b] |
|---|---|---|---|---|---|---|---|---|---|
| GEOS-Chem[a] | **Experiment A** | 8.3 | 0.068 | 0.32 | 0.24 | 9.9 | - 5.3 | 0.15* | 2006-2009 |
| | **Experiment B** | 8.5 | 0.115 | 0.38 | 0.27 | 9.5 | - 2.5 | 0.24* | 2006-2009 |
| | **Experiment C** | 8.5 | 0.115 | 0.37 | 0.25 | 9.2 | - 2.9 | 0.23* | 2006-2009 |
| | **Experiment D** | 8.5 | 0.115 | 0.37 | 0.43 | 16.3 | - 0.8 | 0.21* | 2006-2009 |
| | **Exp. D_ 50% precip.** | 8.5 | 0.115 | 0.31 | 0.48 | 20.7 | +5.8 | 0.22* | 2006-2009 |
| | **Exp. D_200% precip.** | 8.5 | 0.115 | 0.40 | 0.37 | 12.6 | -4.4 | 0.20* | 2006-2009 |
| **AeroCom Phase I[f]** | | 7.8 | 0.069 | 0.11-0.22 | - | - | -13.2~-0.5[g] | 0.11-0.28 | - |
| AeroCom Phase II | **HADGEM2** | 6.6 | 0.063 | 0.34 | 0.34 | 22.6 | + 18.7 | 0.18* | 2006-2008 |
| | **GOCART** | 10.3 | 0.058 | 0.29 | 0.14 | 16.0 | + 7.3 | 0.04 | 2006 |
| | **OsloCTM2** | 7.8 | 0.068 | 0.28 | 0.07 | 6.9 | + 21.4 | 0.10* | 2006 |
| | **GISS-modelE** | 7.6 | 0.077 | 0.22 | 0.16 | 11.6 | + 7.8 | 0.21* | 2004-2008 |
| | **SPRINTARS** | 8.1 | 0.037 | 0.22 | 0.08 | 6.9 | + 5.3 | 0.06 | 2006 |
| | **CAM4-Oslo** | 10.6 | 0.056 | 0.21 | 0.20 | 22.7 | - 0.2 | 0.12* | Present-day |
| | **GMI** | 7.8 | 0.059 | 0.20 | 0.08 | 7.7 | + 1.9 | 0.10* | 2006 |
| | **IMPACT** | 10.6 | 0.039 | 0.16 | 0.05 | - | + 3.8 | 0.18* | Present-day |
| | **CAM5.1** | 7.8 | 0.056 | 0.13 | 0.02 | - | - 13.0 | 0.23* | 2006 |

[a]This study

[b]AeroCom model results are from Jiao *et al.* (2014).

[c]AeroCom models simulated Arctic Burdens are for year 2000 using only anthropogenic emissions from Samset *et al.* (2013)

[d]Lifetime is approximated by dividing the annual Arctic BC column burden by the annual Arctic deposition flux.

[e]BC snow concentrations were calculated using CLM4 and CICE4 models with monthly deposition field from AeroCom models (Jiao *et al.*, 2014).

[f]Paticipating models are DlR, GISS, LOA, LSCE, MATCH, MPI-HAM, TM5, UIO-CTM, UIO-GCM,UIO-GCM-V2, ULAQ, UMI, CAM-Oslo (Jiao *et al.*, 2014)

[g]This range is for the AeroCom Phase I models except for ULAQ, which is the only one produce a positive bias of +10.7 ng g$^{-1}$.

*The regression is significant at $\alpha$=0.05

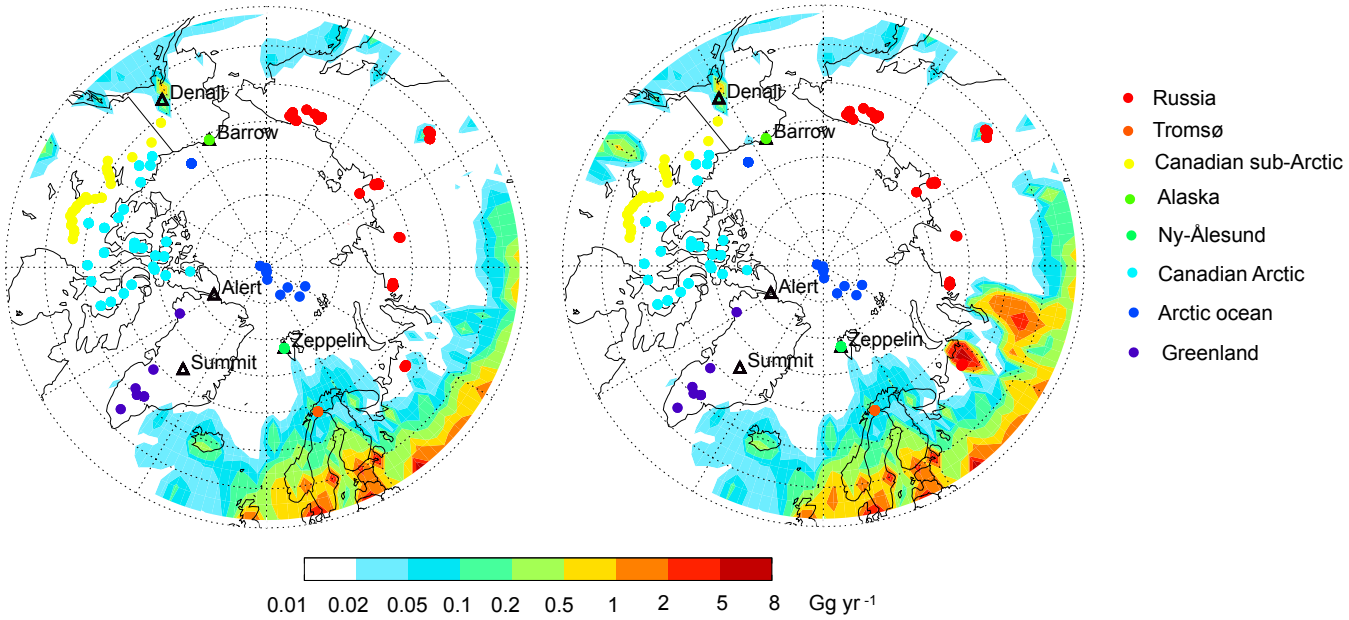


**Figure 1: Annual BC emissions (Gg yr$^{-1}$) in the Arctic in Experiment A (left panel) and Experiments B, C and D (right panel). Also shown are in-situ BC measurement stations (open triangles) and snow sample locations (solid circles). The eight sub-regions of the Arctic as defined in Doherty *et al.* (2010) are color-coded. See text for details.**

5

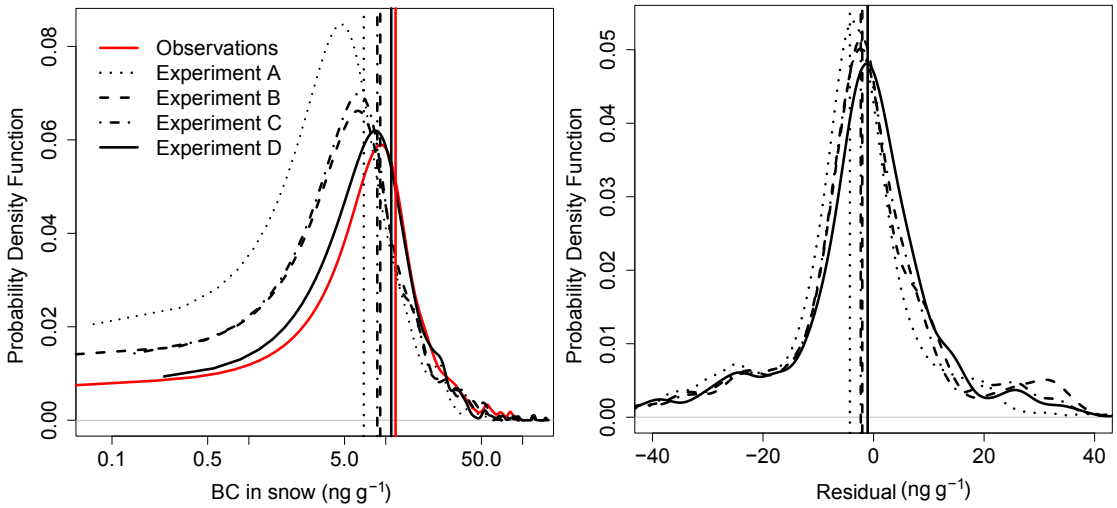


**Figure 2: Probability density function of observed (solid red) and GEOS-Chem simulated (black curves: dotted−Experiment A; dashed−Experiment B; dash dotted−Experiment C; solid−Experiment D, see Table 2 and text for details) BC concentration in snow (ng g$^{-1}$) in the Arctic (left panel), medians (vertical lines, left panel), residual errors (model−observation, right panel) and mean residual errors (vertical lines, right panel).**

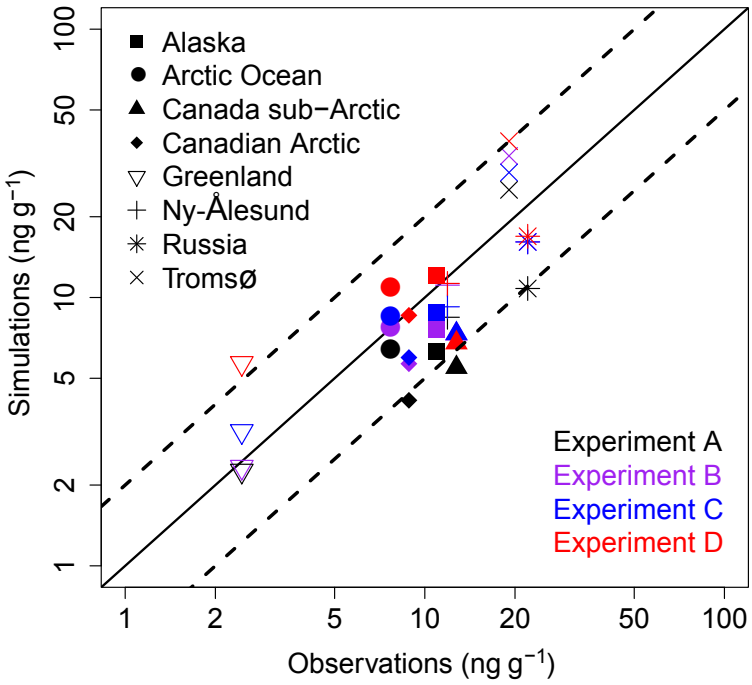


**Figure 3: Observed and GEOS-Chem simulated median BC concentration in snow (ng g$^{-1}$) in the eight sub-regions in the Arctic (see Fig. 1). Solid line is 1:1 ratio line and dashed lines are 1:2 (or 2:1).**

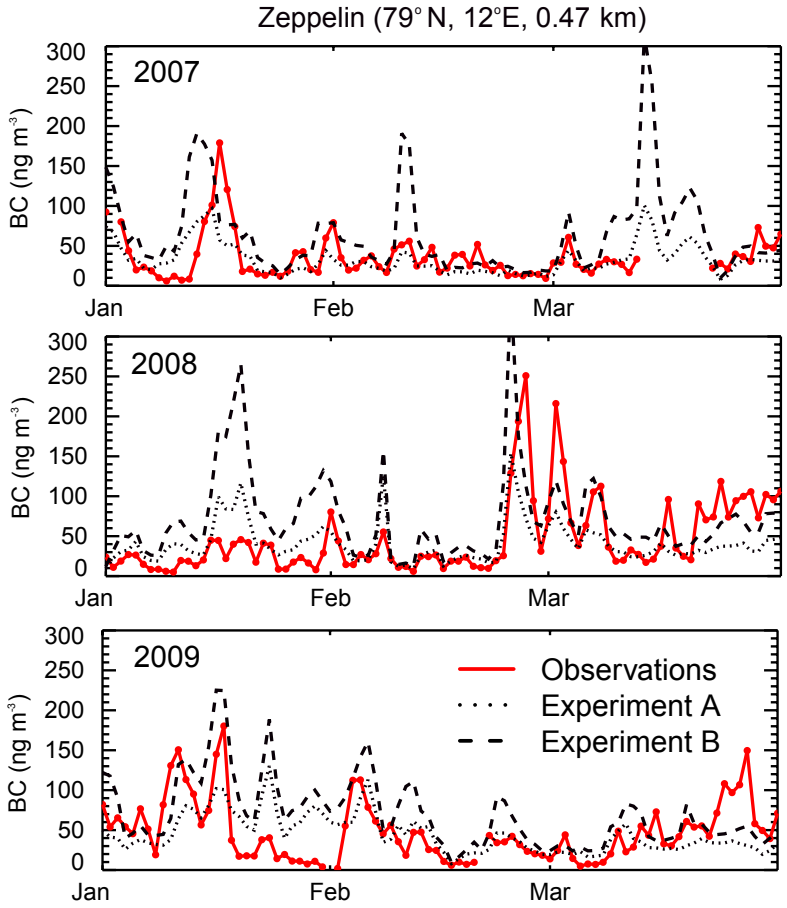


**Figure 4: Observed (red solid) and GEOS-Chem simulated (dotted−Exp. A, dashed−Exp. B, see Table 2 and text for details) daily BC concentrations in air (ng $m^{-3}$) at Zeppelin from January–March in 2007−09.**

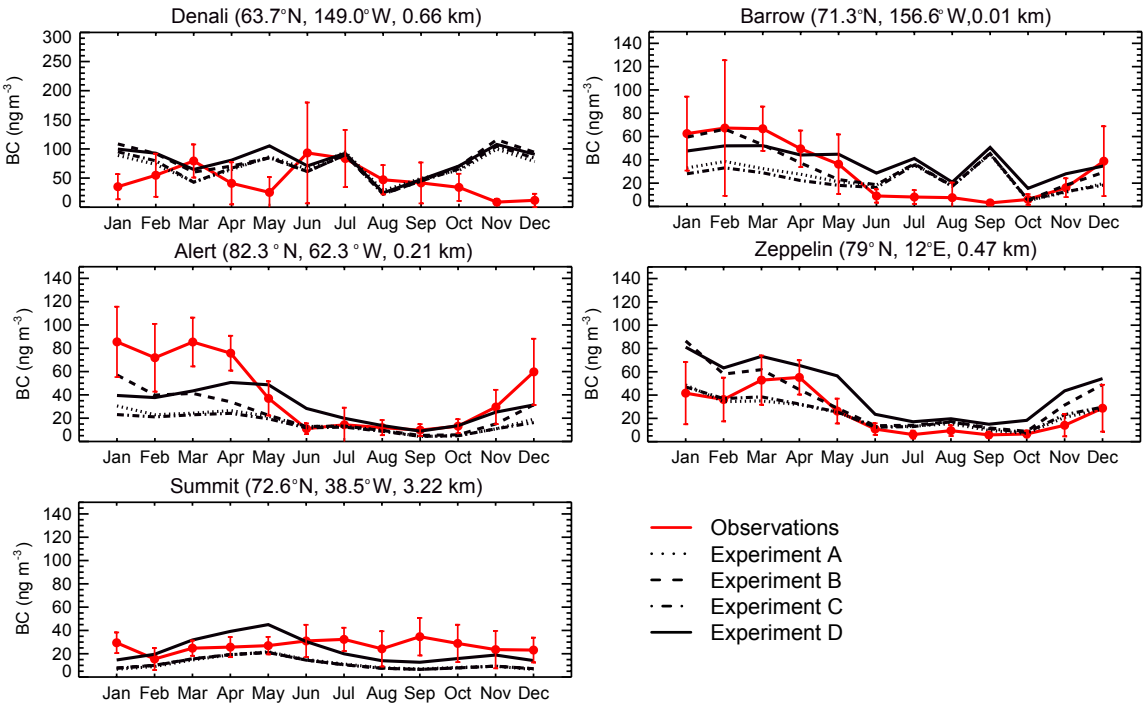


**Figure 5: Observed (red solid) and GEOS-Chem simulated (black curves: dotted−Exp. A, dashed−Exp. B, dash dotted−Exp. C, solid−Exp. D, see Table 2 and text for details) BC concentrations in air (ng m$^{-3}$) at Denali, Barrow, Alert, Zeppelin, and Summit, averaged for 2007−09. Also shown are standard deviations of observations (error bars).**

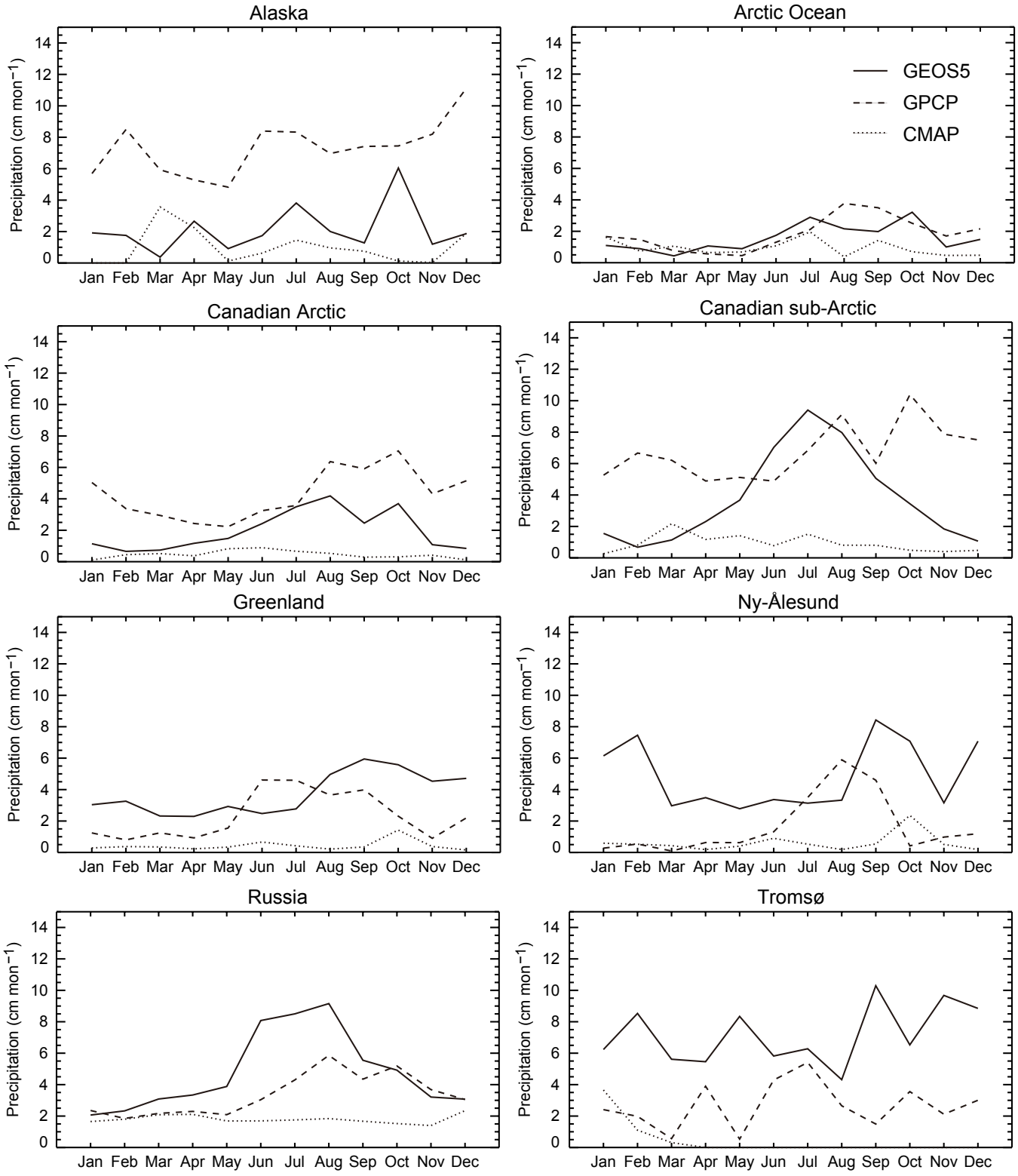


**Figure 6: Monthly precipitation (cm mon$^{-1}$) averaged over sub-regions in the Arctic for 2006−08 (Fig. 1). Data are from the Goddard Earth Observing System Model version 5 data assimilation system (GEOS-5 DAS), Global Precipitation Climatology Project (GPCP), and NOAA Climate Prediction Center Merged Analysis of Precipitation (CMAP).**

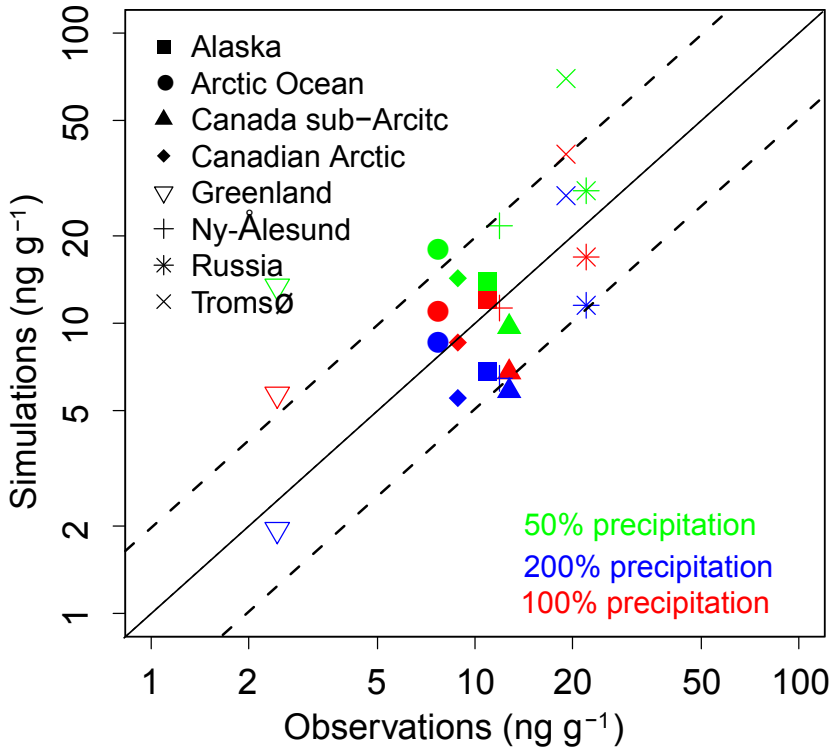


**Figure 7: Same as Fig. 3, but for Exp. D with standard precipitation (red symbols), 50% precipitation (green symbols), and 200% precipitation (blue symbols). See text for details.**

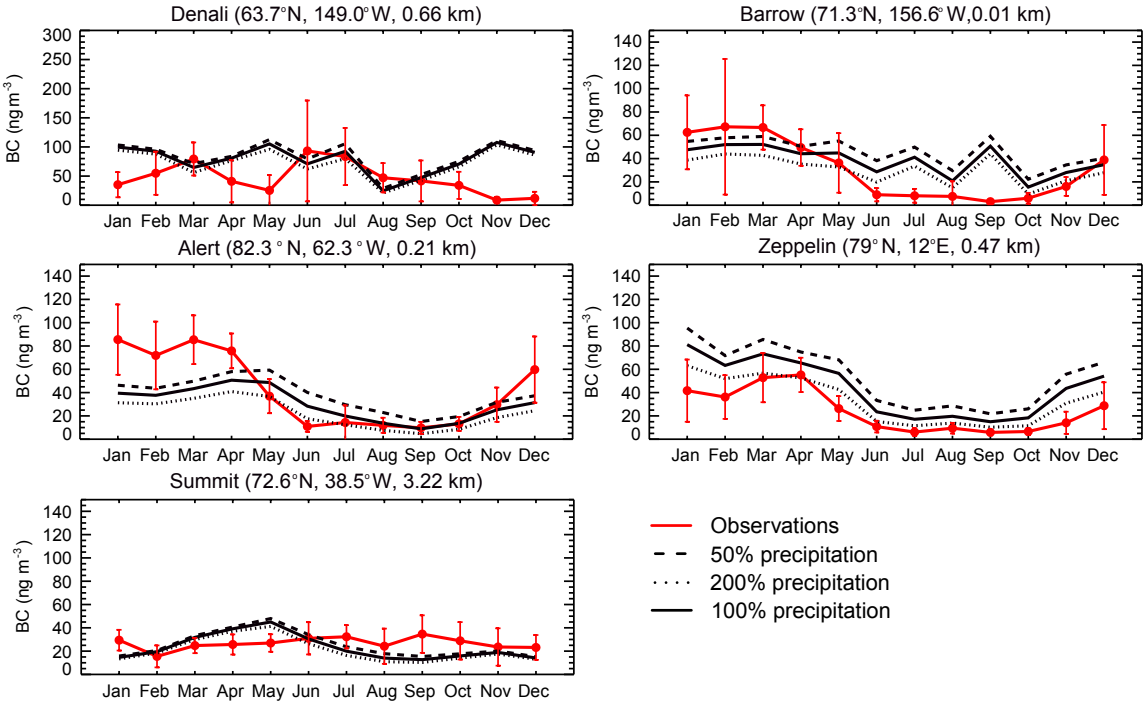


**Figure 8: Same as Fig. 5, but for Exp. D with standard precipitation (solid black), 50% precipitation (dashed black), and 200% precipitation (dotted black). See text for details.**